Appendix A. Supplementary data

Supplementary data associated with this article can be found, in the online version, at doi:10.1016/j.expneurol.2009.05.001.

References

Amir, R.E., Zoghbi, H.Y., 2000. Rett syndrome: methyl-CpG-binding protein 2 mutations and phenotype-genotype correlations. Am. J. Med. Genet. 97, 147–152.

Amir, R.E., Van den Veyver, I.B., Wan, M., Tran, C.Q., Francke, U., Zoghbi, H.Y., 1999. Rett syndrome is caused by mutations in X-linked MECP2, encoding methyl-CpG-binding protein 2. Nat. Genet. 23, 185–188.

Avruch, J., 1998. Insulin signal transduction through protein kinase cascades. Mol. Cell. Biochem. 182, 31–48.

Bird, A., 2002. DNA methylation patterns and epigenetic memory. Genes Dev. 16, 6–21.

Bonni, A., Sun, Y., Nadal-Vicens, M., Bhatt, A., Frank, D.A., Rozovsky, I., Stahl, N., Yancopoulos, G.D., Greenberg, M.E., 1997. Regulation of gliogenesis in the central nervous system by the JAK-STAT signaling pathway. Science 278, 477–483.

Brami-Cherrier, K., Valjent, E., Herve, D., Darragh, J., Corvol, J.C., Pages, C., Arthur, S.J., Girault, J.A., Caboche, J., 2005. Parsing molecular and behavioral effects of cocaine in mitogen- and stress-activated protein kinase-1-deficient mice. J. Neurosci. 25, 11444–11454.

Cao, Q.L., Zhang, Y.P., Howard, R.M., Walters, W.M., Tsoulfas, P., Whittemore, S.R., 2001. Pluripotent stem cells engrafted into the normal or lesioned adult rat spinal cord are restricted to a glial lineage. Exp. Neurol. 167, 48–58.

Chahrour, M., Jung, S.Y., Shaw, C., Zhou, X., Wong, S.T., Qin, J., Zoghbi, H.Y., 2008. MeCP2, a key contributor to neurological disease, activates and represses transcription. Science 320, 1224–1229.

Chao, H.T., Zoghbi, H.Y., Rosenmund, C., 2007. MeCP2 controls excitatory synaptic strength by regulating glutamatergic synapse number. Neuron 56, 58–65.

Chen, R.Z., Akbarian, S., Tudor, M., Jaenisch, R., 2001. Deficiency of methyl-CpG binding protein-2 in CNS neurons results in a Rett-like phenotype in mice. Nat. Genet. 27, 327–331.

Chong, J.A., Tapia-Ramirez, J., Kim, S., Toledo-Aral, J.J., Zheng, Y., Boutros, M.C., Altshuller, Y.M., Frohman, M.A., Kraner, S.D., Mandel, G., 1995. REST: a mammalian silencer protein that restricts sodium channel gene expression to neurons. Cell 80, 949–957.

Colantuoni, C., Jeon, O.H., Hyder, K., Chenchik, A., Khimani, A.H., Narayanan, V., Hoffman, E.P., Kaufmann, W.E., Naidu, S., Pevsner, J., 2001. Gene expression profiling in postmortem Rett syndrome brain: differential gene expression and patient classification. Neurobiol. Dis. 8, 847–865.

Collins, A.L., Levenson, J.M., Vilaythong, A.P., Richman, R., Armstrong, D.L., Noebels, J.L., David Sweatt, J., Zoghbi, H.Y., 2004. Mild overexpression of MeCP2 causes a progressive neurological disorder in mice. Hum. Mol. Genet. 13, 2679–2689.

Conti, L., Pollard, S.M., Gorba, T., Reitano, E., Toselli, M., Biella, G., Sun, Y., Sanzone, S., Ying, Q.L., Cattaneo, E., Smith, A., 2005. Niche-independent symmetrical self-renewal of a mammalian tissue stem cell. PLoS Biol. 3, e283.

Edlund, T., Jessell, T.M., 1999. Progression from extrinsic to intrinsic signaling in cell fate specification: a view from the nervous system. Cell 96, 211–224.

Fan, G., Martinowich, K., Chin, M.H., He, F., Fouse, S.D., Hutnick, L., Hattori, D., Ge, W., Shen, Y., Wu, H., ten Hoeve, J., Shuai, K., Sun, Y.E., 2005. DNA methylation controls the timing of astrogliogenesis through regulation of JAK-STAT signaling. Development 132, 3345–3356.

Gage, F.H., 2000. Mammalian neural stem cells. Science 287, 1433–1438.

Gomes, W.A., Mehler, M.F., Kessler, J.A., 2003. Transgenic overexpression of BMP4 increases astroglial and decreases oligodendroglial lineage commitment. Dev. Biol. 255, 164–177.

Gross, R.E., Mehler, M.F., Mabie, P.C., Zang, Z., Santschi, L., Kessler, J.A., 1996. Bone morphogenetic proteins promote astroglial lineage commitment by mammalian subventricular zone progenitor cells. Neuron 17, 595–606.

Hofstetter, C.P., Holmstrom, N.A., Lilja, J.A., Schweinhardt, P., Hao, J., Spenger, C., Wiesenfeld-Hallin, Z., Kurpad, S.N., Frisen, J., Olson, L., 2005. Allodynia limits the usefulness of intraspinal neural stem cell grafts; directed differentiation improves outcome. Nat. Neurosci. 8, 346–353.

Hsieh, J., Gage, F.H., 2004. Epigenetic control of neural stem cell fate. Curr. Opin. Genet. Dev. 14, 461–469.

Johansson, C.B., Momma, S., Clarke, D.L., Risling, M., Lendahl, U., Frisen, J., 1999. Identification of a neural stem cell in the adult mammalian central nervous system. Cell 96, 25–34.

Jones, P.L., Veenstra, G.J., Wade, P.A., Vermaak, D., Kass, S.U., Landsberger, N., Strouboulis, J., Wolffe, A.P., 1998. Methylated DNA and MeCP2 recruit histone deacetylase to repress transcription. Nat. Genet. 19, 187–191.

Jung, B.P., Zhang, G., Ho, W., Francis, J., Eubanks, J.H., 2002. Transient forebrain ischemia alters the mRNA expression of methyl DNA-binding factors in the adult rat hippocampus. Neuroscience 115, 515–524.

Kishi, N., Macklis, J.D., 2004. MECP2 is progressively expressed in post-migratory neurons and is involved in neuronal maturation rather than cell fate decisions. Mol. Cell. Neurosci. 27, 306–321.

Klose, R.J., Bird, A.P., 2006. Genomic DNA methylation: the mark and its mediators. Trends Biochem. Sci. 31, 89–97.

Kohyama, J., Kojima, T., Takatsuka, E., Yamashita, T., Namiki, J., Hsieh, J., Gage, F.H., Namihira, M., Okano, H., Sawamoto, K., Nakashima, K., 2008. Epigenetic regulation of neural cell differentiation plasticity in the adult mammalian brain. Proc. Natl. Acad. Sci. U. S. A. 105, 18012–18017.

Kouhara, H., Hadari, Y.R., Spivak-Kroizman, T., Schilling, J., Bar-Sagi, D., Lax, I., Schlessinger, J., 1997. A lipid-anchored Grb2-binding protein that links FGF-receptor activation to the Ras/MAPK signaling pathway. Cell 89, 693–702.

Lim, D.A., Tramontin, A.D., Trevejo, J.M., Herrera, D.G., Garcia-Verdugo, J.M., Alvarez-Buylla, A., 2000. Noggin antagonizes BMP signaling to create a niche for adult neurogenesis. Neuron 28, 713–726.

Meehan, R.R., Lewis, J.D., Bird, A.P., 1992. Characterization of MeCP2, a vertebrate DNA binding protein with affinity for methylated DNA. Nucleic Acids Res. 20, 5085–5092.

Menard, C., Hein, P., Paquin, A., Savelson, A., Yang, X.M., Lederfein, D., Barnabe-Heider, F., Mir, A.A., Sterneck, E., Peterson, A.C., Johnson, P.F., Vinson, C., Miller, F.D., 2002. An essential role for a MEK-C/EBP pathway during growth factor-regulated cortical neurogenesis. Neuron 36, 597–610.

Morita, S., Kojima, T., Kitamura, T., 2000. Plat-E: an efficient and stable system for transient packaging of retroviruses. Gene. Ther. 7, 1063–1066.

Nakamura, M., Houghtling, R.A., MacArthur, L., Bayer, B.M., Bregman, B.S., 2003. Differences in cytokine gene expression profile between acute and secondary injury in adult rat spinal cord. Exp. Neurol. 184, 313–325.

Nakashima, K., Wiese, S., Yanagisawa, M., Arakawa, H., Kimura, N., Hisatsune, T., Yoshida, K., Kishimoto, T., Sendtner, M., Taga, T., 1999a. Developmental requirement of gp130 signaling in neuronal survival and astrocyte differentiation. J. Neurosci. 19, 5429–5434.

Nakashima, K., Yanagisawa, M., Arakawa, H., Kimura, N., Hisatsune, T., Kawabata, M., Miyazono, K., Taga, T., 1999b. Synergistic signaling in fetal brain by STAT3-Smad1 complex bridged by p300. Science 284, 479–482.

Nakashima, K., Takizawa, T., Ochiai, W., Yanagisawa, M., Hisatsune, T., Nakafuku, M., Miyazono, K., Kishimoto, T., Kageyama, R., Taga, T., 2001. BMP2-mediated alteration in the developmental pathway of fetal mouse brain cells from neurogenesis to astrocytogenesis. Proc. Natl. Acad. Sci. U. S. A. 98, 5868–5873.

Namihira, M., Nakashima, K., Taga, T., 2004. Developmental stage dependent regulation of DNA methylation and chromatin modification in a immature astrocyte specific gene promoter. FEBS Lett. 572, 184–188.

Namihira, M., Kohyama, J., Semi, K., Sanosaka, T., Deneen, B., Taga, T., Nakashima, K., 2009. Committed neuronal precursors confer astrocytic potential on residual neural precursor cells. Dev. Cell. 16, 245–255.

Namiki, J., Tator, C.H., 1999. Cell proliferation and nestin expression in the ependyma of the adult rat spinal cord after injury. J. Neuropathol. Exp. Neurol. 58, 489–498.

Nan, X., Ng, H.H., Johnson, C.A., Laherty, C.D., Turner, B.M., Eisenman, R.N., Bird, A., 1998. Transcriptional repression by the methyl-CpG-binding protein MeCP2 involves a histone deacetylase complex. Nature 393, 386–389.

Ogawa, Y., Sawamoto, K., Miyata, T., Miyao, S., Watanabe, M., Nakamura, M., Bregman, B.S., Koike, M., Uchiyama, Y., Toyama, Y., Okano, H., 2002. Transplantation of in vitro-expanded fetal neural progenitor cells results in neurogenesis and functional recovery after spinal cord contusion injury in adult rats. J. Neurosci. Res. 69, 925–933.

Paquin, A., Barnabe-Heider, F., Kageyama, R., Miller, F.D., 2005. CCAAT/enhancer-binding protein phosphorylation biases cortical precursors to generate neurons rather than astrocytes in vivo. J. Neurosci. 25, 10747–10758.

Pollard, S.M., Conti, L., Sun, Y., Goffredo, D., Smith, A., 2006. Adherent neural stem (NS) cells from fetal and adult forebrain. Cereb. Cortex 16 (Suppl. 1), i112–i120.

Qian, X., Shen, Q., Goderie, S.K., He, W., Capela, A., Davis, A.A., Temple, S., 2000. Timing of CNS cell generation: a programmed sequence of neuron and glial cell production from isolated murine cortical stem cells. Neuron 28, 69–80.

Rajan, P., McKay, R.D., 1998. Multiple routes to astrocytic differentiation in the CNS. J. Neurosci. 18, 3620–3629.

Schoenherr, C.J., Anderson, D.J., 1995. The neuron-restrictive silencer factor (NRSF): a coordinate repressor of multiple neuron-specific genes. Science 267, 1360–1363.

Setoguchi, T., Nakashima, K., Takizawa, T., Yanagisawa, M., Ochiai, W., Okabe, M., Yone, K., Komiya, S., Taga, T., 2004. Treatment of spinal cord injury by transplantation of fetal neural precursor cells engineered to express BMP inhibitor. Exp. Neurol. 189, 33–44.

Setoguchi, H., Namihira, M., Kohyama, J., Asano, H., Sanosaka, T., Nakashima, K., 2006. Methyl-CpG binding proteins are involved in restricting differentiation plasticity in neurons. J. Neurosci. Res. 84, 969–979.

Shahbazian, M.D., Antalffy, B., Armstrong, D.L., Zoghbi, H.Y., 2002. Insight into Rett syndrome: MeCP2 levels display tissue- and cell-specific differences and correlate with neuronal maturation. Hum. Mol. Genet. 11, 115–124.

Stancheva, I., Collins, A.L., Van den Veyver, I.B., Zoghbi, H., Meehan, R.R., 2003. A mutant form of MeCP2 protein associated with human Rett syndrome cannot be displaced from methylated DNA by notch in *Xenopus* embryos. Mol. Cell. 12, 425–435.

Sun, Y., Nadal-Vicens, M., Misono, S., Lin, M.Z., Zubiaga, A., Hua, X., Fan, G., Greenberg, M. E., 2001. Neurogenin promotes neurogenesis and inhibits glial differentiation by independent mechanisms. Cell 104, 365–376.

Takizawa, T., Nakashima, K., Namihira, M., Ochiai, W., Uemura, A., Yanagisawa, M., Fujita, N., Nakao, M., Taga, T., 2001. DNA methylation is a critical cell-intrinsic determinant of astrocyte differentiation in the fetal brain. Dev. Cell. 1, 749–758.

Vroemen, M., Aigner, L., Winkler, J., Weidner, N., 2003. Adult neural progenitor cell grafts survive after acute spinal cord injury and integrate along axonal pathways. Eur. J. Neurosci. 18, 743–751.

Zhou, Z., Hong, E.J., Cohen, S., Zhao, W.N., Ho, H.Y., Schmidt, L., Chen, W.G., Lin, Y., Savner, E., Griffith, E.C., Hu, L., Steen, J.A., Weitz, C.J., Greenberg, M.E., 2006. Brain-specific phosphorylation of MeCP2 regulates activity-dependent Bdnf transcription, dendritic growth, and spine maturation. Neuron 52, 255–269.

The Journal of Immunology

CD72 Negatively Regulates KIT-Mediated Responses in Human Mast Cells

Tatsuki R. Kataoka, Atsushi Kumanogoh, Geethani Bandara, Dean D. Metcalfe and Alasdair M. Gilfillan

J. Immunol. 2010;184;2468-2475; originally published online Jan 25, 2010;
doi:10.4049/jimmunol.0902450
http://www.jimmunol.org/cgi/content/full/184/5/2468

The Journal of Immunology is published twice each month by The American Association of Immunologists, Inc., 9650 Rockville Pike, Bethesda, MD 20814-3994.

Print ISSN: 0022-1767 Online ISSN: 1550-6606.

CD72 Negatively Regulates KIT-Mediated Responses in Human Mast Cells

Tatsuki R. Kataoka,*,† Atsushi Kumanogoh,‡,§ Geethani Bandara,* Dean D. Metcalfe,* and Alasdair M. Gilfillan*

KIT activation, through binding of its ligand, stem cell factor, is crucial for normal mast cell growth, differentiation, and survival. Furthermore, KIT may also contribute to mast cell homing and cytokine generation. Activating mutations in KIT lead to the dysregulated mast cell growth associated with the myeloproliferative disorder, mastocytosis. We investigated the potential of downregulating such responses through mast cell inhibitory receptor activation. In this study, we report that the B cell-associated ITIM-containing inhibitory receptor, CD72, is expressed in human mast cells. Ligation of CD72 with the agonistic Ab, BU40, or with recombinant human CD100 (rCD100), its natural ligand, induced the phosphorylation of CD72 with a resulting increase in its association with the tyrosine phosphatase SH2 domain-containing phosphatase-1. This, in turn, resulted in an inhibition of KIT-induced phosphorylation of Src family kinases and extracellular-regulated kinases (ERK1/2). As a consequence of these effects, KIT-mediated mast cell proliferation, chemotaxis, and chemokine production were significantly reduced by BU40 and rCD100. Furthermore, BU40 and rCD100 also downregulated the growth of the HMC1.2 human mast cell line. Thus, targeting CD72 may provide a novel approach to the suppression of mast cell disease such as mastocytosis. *The Journal of Immunology*, **2010, 184: 2468–2475.**

Mast cells are cells of hematopoietic lineage that participate in both innate and acquired immune responses (1). The activation of KIT by its ligand, stem cell factor (SCF, also termed steel factor or KIT ligand), initiates signaling cascades that are critical for mast cell growth, development, and survival (2). Furthermore, these signals also induce mast cell chemotaxis and, at least under experimental conditions, adhesion (2). Gain of function mutations in KIT lead to the dysregulated cell growth associated with the clonal accumulation of mast cells in tissues as observed in systemic mastocytosis and mast cell leukemia (3–5).

KIT-mediated responses in mast cells, however, can be modified by signals produced by other receptors expressed on the cell surface (6–8). For example, the ability of KIT to promote mast cell growth can be markedly enhanced by IL-3–induced ligation of the IL-3 receptor (2). In contrast, mast cells also express surface receptors, including FcγRIIb, Siglecs, mast cell function-associated Ag (MAFA), signal regulatory protein α, leukocyte Ig-like receptor B4 (formerly gp49B1), paired Ig-like receptor-B, myeloid-associated Ig-like receptor I, CD200 receptor, and CD300a, which have the capacity to downregulate such activation (9–11). These inhibitory receptors are largely typified by ITIMs within their cytosolic domains (9). ITIMs comprise the homology sequence (I/V/L/S)xYxx(L/V) (x is any residue) (12). On receptor ligation/activation, the tyrosines contained within these sequences become phosphorylated after the activation of receptor tyrosine kinases or Src family member tyrosine kinases (SFKs). This allows the recruitment of the nonreceptor protein phosphatases, Src homology 2 domain-containing tyrosine phosphatase (SHP)-1, SHP-2, or Src homology 2 domain-containing inositol 5-phosphatase (SHIP) 1 (12). SHP-1 and SHP-2 are tyrosine phosphatases that dephosphorylate tyrosine-containing signaling molecules, thereby reversing the action of tyrosine kinases, whereas SHIP1 dephosphorylates phospatidylinositol 3,4,5 trisphosphate at the 3′ position thereby terminating PI3K-driven signaling pathways (12). ITIM-containing receptors, thus, may have application in the management of mast cell-driven disease. However, in many cases the natural ligands for the inhibitory receptors are unknown (9) and those that are known may not be ideal for downregulating mast cell responses. For these reasons, downregulation of mast cell responses via inhibitory receptors has primarily been achieved using Abs targeting the receptors.

We, therefore, wished to explore whether we could downregulate KIT-mediated mast cell responses through an ITIM-bearing inhibitory receptor using its recognized soluble ligand. One such receptor is CD72 (Lyb-2), an ITIM-containing, 45 kDa type II transmembrane protein of the C type lectin family (13) whose natural ligand has been identified as CD100 or Semaphorin 4D (Sema4D) (14). In this study, we report that CD72 is expressed on human mast cells (huMCs) derived from CD34-positive peripheral blood cells of healthy volunteers and huMC lines. The concurrent ligation of CD72 and KIT resulted in an increase in the phosphorylation of CD72, and enhanced association between CD72 and SHP-1. This led to the suppression of the KIT-mediated phosphorylation of SFKs and ERKs, critical players in KIT-mediated huMC responses (6). Thus, ligation of CD72 reduced KIT-mediated proliferation, chemotaxis, and MCP-1 (CCL2) production in huMCs and the suppression of growth of HMC1.2 cells harboring the gain-of-function mutation in KIT gene. From these studies, we conclude that CD72–CD100 interactions downregulate KIT-mediated mast cell responses via the formation of the

*Laboratory of Allergic Diseases, National Institute of Allergy and Infectious Diseases, National Institutes of Health, Bethesda, MD 20892; †Department of Pathology, Hyogo College of Medicine, Nishinomiya, Hyogo; ‡Department of Immunopathology, Research Institute for Microbial Diseases; and §WPI Immunology Frontier Research Center, Osaka University, Suita, Osaka, Japan

Received for publication July 28, 2009. Accepted for publication December 28, 2009.

This work was supported by the National Institute of Allergy and Infectious Diseases Division of Intramural Research within the National Institutes of Health, United States, and by grants from the Ministry of Education, Culture, Sports, Science and Technology, Japan.

Address correspondence and request reprints to Dr. Tatsuki R. Kataoka, Department of Pathology, Hyogo College of Medicine, 1-1, Mukogawa, Nishinomiya, Hyogo, 663-8501, Japan. E-mail address: trkataoka@yahoo.co.jp

Abbreviations used in this paper: β-hex, β-hexominidase; huMC, human mast cell; MAFA, mast cell function-associated Ag; rCD100, recombinant human CD100; SCF, stem cell factor; SFK, Src family member tyrosine kinases; SHIP, Src homology 2 domain-containing inositol 5-phosphatase; SHP, Src homology 2 domain-containing tyrosine phosphatase; Stat3, signal transducers and activators of transcription 3.

www.jimmunol.org/cgi/doi/10.4049/jimmunol.0902450

CD72–SHP-1 complex. Thus, downregulation of KIT-mediated responses through CD72 may provide a potential means for the control of mast cell-driven disorders.

Materials and Methods

Cells

The huMCs, derived from CD34-positive peripheral blood cells, were cultured in StemPro-34 medium with supplement (Invitrogen, Carlsbad, CA), containing L-glutamine (2 mM), penicillin (100 U/ml), streptomycin (100 μg/ml), recombinant human SCF (100 ng/ml, Peprotech, Rocky Hill, NJ), and recombinant human IL-6 (100 ng/ml, Peprotech) as before (15). The human LAD2 mast cell line was cultured in StemPro-34 with supplement containing L-glutamine (2 mM), penicillin (100 U/ml), streptomycin (100 μg/ml), and recombinant human SCF (100 ng/ml, Peprotech) (16). HMC1.1 (expresses V560G KIT) and HMC1.2 (expresses V560G and D816V KIT) huMC lines were grown in IMDM medium supplemented with FBS (10%), L-glutamine (2 mM), penicillin (100 U/ml), and streptomycin (100 μg/ml) (5, 17, 18). The U937 monocytic cell line and the Raji human B cell line were purchased from American Type Culture Collection (Manassas, VA), and grown in RPMI 1640 medium supplemented with FBS (10%), L-glutamine (2 mM), penicillin (100 U/ml), and streptomycin (100 μg/ml).

Recombinant CD100 and Abs

Recombinant CD100 (rCD100) protein was prepared as described (19). The anti-human CD72 Ab BU40 (monoclonal, mouse IgG) was purchased from Southern Biotechnology Associates (Birmingham, AL). The anti-CD72 Ab H-96 (rabbit polyclonal IgG) and anti–SHP-1 Ab (C-19, rabbit polyclonal IgG) were purchased from Santa Cruz Biotechnology (Santa Cruz, CA). Anti-phosphotyrosine Ab (4G10, mouse monoclonal IgG) was purchased from Millipore (Billerica, MA). Anti–phospho-KIT (Tyr 703) Ab (rabbit polyclonal IgG) was purchased from Invitrogen. Anti–phospho-Src (Tyr 416) and anti–phospho-ERK Ab (both Abs were rabbit polyclonal IgG) were obtained from Cell Signaling Technology (Beverly, MA). Anti-β-actin Ab (mouse monoclonal IgG) was obtained from Sigma-Aldrich (St. Louis, MO). Isotype control Abs were obtained from BD Biosciences (San Jose, CA) and the secondary Abs were peroxidase-labeled anti-rabbit or anti-mouse IgG Abs from Santa Cruz Biotechnology.

Immunoblotting and immunoprecipitation

Cell lysates were prepared, the proteins separated by electrophoresis, and gels probed for immunoreactive proteins as described (20). Immunoprecipitation experiments were executed using an anti-CD72 Ab (H-96) or anti–SHP-1 Ab (C-19) as described (19). The cells were lysed with buffer containing 150 mM NaCl, 10 mM Tris-HCl (pH 8.0), 1 mM EDTA, 1 mM Na_3VO_4, 0.5 mM PMSF, 5 μg/ml aprotinin, 5 μg/ml leupeptin, Complete protease inhibitor cocktails (Roche, Indianapolis, IN), and NP-40 (1%). The cell lysates were incubated with rabbit IgG-bound protein G-Sepharose for 30 min, then incubated with anti-CD72 Ab (H-96)-bound or anti–SHP-1 Ab (C-19)-bound protein G-Sepharose overnight at 4°C with rotation.

RT-PCR

Total RNA was extracted from 5×10^5 cells (huMCs at various times of culture, LAD2, HMC1.1, HMC1.2, U937, and Raji). Cells were lysed with Trizol (Invitrogen) and RNA was extracted using Rneasy Mini Kit (Qiagen, Valencia CA). cDNA was synthesized and amplified using SuperScript III One-Step RT-PCR System (Invitrogen). One microgram of RNA was used for cDNA synthesis. A 834-bp region of CD72 gene between exon1–6 was amplified using the primers 5′-ATGGCTGAGGCCATCACCTA-3′, and 5′-TGATTGTGGATAAATTTCACTGAAT-3′ and a 998-bp fragment between exon 2–8 was amplified using primers 5′-ACCCAGGGGCTGATGAT-3′ and 5′-CTAATCTGGAAACCTGAAAGCTG-3′. cDNA synthesis and PCR amplification were performed with a DNA Engine PTC200 cycler (Bio Rad Laboratories, Hercules, CA) with the following thermal cycle protocol: 50°C for 30 min, 94°C for 2 min, followed by 30 cycles of 94°C for 30 s, 60°C for 1 min, 72°C for 1 min, and a final extension of 10 min at 72°C.

Flow cytometry

For the detection of CD72 surface expression, huMCs, LAD2, HMC1.1, or HMC1.2 cells were washed with PBS, and fixed with 4% paraformaldehyde (Sigma-Aldrich). The cells were stained with anti-human CD72 (BU40) overnight at 4°C, followed by anti-mouse IgG-FITC for 2 h at 4°C. The cells were then analyzed using a FACScan flow cytometer.

Cell cycle analysis

Cell cycle progression of huMCs or HMC1.2 was analyzed as described (21). Briefly, huMCs or HMC1.2 cells were cultured overnight in cytokine-free medium, and resuspended in HEPES buffer containing 0.04% BSA (huMCs) or IMEM and 10% FBS (HMC1.2). After 30 min preculture, 10 ng/ml SCF was added and the cells cultured for 30 min with or without control IgG, BU40, or rCD100 (10 μg/ml, respectively). The cells were fixed with 100% ethanol, treated with RNase A (Roche), and stained with propidium iodine (Sigma-Aldrich) for 2 h at 4°C. The cells were then analyzed using a FACScan flow cytometer.

BrdU cell proliferation assay

Cell proliferation was determined by the BrdU (an analog of thymidine) assay that measures its incorporation into DNA. HuMCs were cultured overnight in cytokine-free StemPro-34 medium, then resupended in the same medium. HuMCs were then incubated for 24 h at 1.5×10^5 cells/100 μl in 96-well plates with PBS with 0.1% NaN_3, SCF and PBS with 0.1% NaN_3, SCF and control IgG (10 μg/ml), SCF and BU40 (10 μg/ml), or SCF and rCD100 (10 μg/ml) (SCF; 10 ng/ml, respectively). HMC1.2 cells were cultured overnight in IMEM without FBS, then resuspended in IMEM containing 10% FBS. HMC1.2 cells were then incubated for 24 h at 1.5×10^5 cells/100 μl in 96-well plates with PBS with 0.1% NaN3, control IgG (10 μg/ml), BU40 (10 μg/ml), or rCD100 (10 μg/ml). Incorporation of BrdU into the huMCs or HMC1.2 cells was assessed using a BrdU cell proliferation assay kit (Calbiochem, San Diego, CA) as previously described (21).

Chemotaxis assay

Chemotaxis was assessed using transwell polycarbonate membranes (8 μm pores, Costar, Cole-Parmer, Vernon Hills, IL) as described (20). Briefly, 1×10^5 huMCs were cultured overnight in cytokine-free medium, and resuspended in HEPES buffer containing 0.5% BSA. PBS with 0.1% NaN3, control IgG (10 μg/ml), BU40 (10 μg/ml), or rCD100 (10 μg/ml) was added to the cell suspension (1×10^5/100 μl), then the cells placed in the upper chamber. The upper chambers were placed in lower chambers containing 600 μl of HEPES buffer with 0.5% BSA for 30 min at 37°C, then chemotaxis was assessed by placing the upper chambers in a new set of lower chambers containing the same buffer with SCF (30 ng/ml). After 4 h incubation at 37°C, the cells migrating to the lower wells were collected and counted by microscopy.

MCP-1 (CCL2) secretion

To examine KIT-mediated MCP-1 (CCL2) secretion (22), huMCs were cultured overnight in cytokine-free medium, then resuspended in cytokine-free medium. A total of 1×10^5 huMCs per 100 μl/well were cultured for 6 h in the presence of 10 ng/ml SCF with or without control IgG, BU40, or rCD100 (10 μg/ml, respectively). The cell-free supernatants (50 μl) were taken for ELISA assay (human MCP-1 DuoSet ELISA system, R&D Systems, Minneapolis, MN) according to the manufacture's protocol.

Degranulation assay

Degranulation from huMCs was monitored by β-hexominidase (β-hex) release as previously described (20). HuMCs were sensitized overnight in cytokine-free, supplemented StemPro cell culture medium containing human myeloma IgE (100 ng/ml, Calbiochem, EMD Bioscienes, San Diego, CA, biotinylated in the National Institutes of Allergy and Infectious Diseases core facility), in the presence of control IgG, BU40, or rCD100 (10 μg/ml, respectively). After rinsing in HEPES buffer containing 0.04% BSA, the cells were activated in this buffer with streptavidin (100 ng/ml, Sigma-Aldrich) with or without SCF (1 ng/ml) for 30 min. The reactions were terminated by centrifugation (3000 rpm for 5 min) at 4°C, and the supernatants were aliquoted to 96-well plates for β-hex assay. The remaining cells were lysed by adding 0.1% Triton X-100, then also analyzed for β-hex content. Degranulation was calculated as percentages of total β-hex content found in the supernatants after challenge.

Statistical analysis

Data were expressed as the mean ± SE. Differences between groups were examined for statistical significance using Student *t* test. A p value <0.05 indicated statistical significance.

Results

HuMCs express CD72

To first explore whether CD72 is expressed in huMCs, we examined the presence of CD72 mRNA in huMCs and the HMC1.1, HMC1.2, and LAD2 huMC lines. Two sets of primers were designed,

targeting exon1 to exon 6, or exon 2 to exon 8, of CD72 mRNA. Raji cells (human Burkitt's lymphoma B cell line) were used as a positive control and U937 cells as a negative control (23). As expected, mRNA for CD72 was found in the Raji cells, but not in the U937 cells (Fig. 1*A*). CD72 mRNA was also detected in primary cultured huMCs, and in the LAD2, HMC1.1, and HMC1.2 huMC lines, with the size of these transcripts being identical to that of the Raji cells (Fig. 1*A*). CD72 mRNA was detected at all times during the development of the huMCs cultures. The CD72 mRNA levels of 1- and 2-wk-old cultures were as high as that of HMC1.2 cells. However, the CD72 mRNA levels tended to decrease during subsequent culture periods (Fig. 1*B*).

To confirm the presence of CD72 in huMCs, we next examined protein expression by immunoblot analysis. These studies verified that CD72 protein is present in the primary cultured huMCs and human tumor mast cell lines, as well as in the Raji control cells (Fig. 1*C*). The expression of CD72 in the HMC1.1 and HMC1.2 cell lines was greater than the expression levels observed in the mature (8 wk) huMCs and LAD2 cells. Again, CD72 protein was absent in the U937 negative control (Fig. 1*C*). To establish that CD72 was expressed at the cell surface, we examined surface staining with an anti-CD72 Ab by FACS analysis. As can be seen from Fig. 1*D*, surface CD72 was detected on both cell types examined; huMCs and HMC1.2 cells.

Concurrent ligation of CD72 and KIT induces CD72 phosphorylation, SHP-1 recruitment, and SHP-1 phosphorylation

Members of the ITIM-bearing family of inhibitory receptors mediate their effects through recruitment of the inositol phosphatases SHIP1 and SHIP2 or the tyrosine phosphates SHP-1 and SHP-2 (12). CD72 contains two ITIMs, one of which binds SHP-1 and the other Grb2, when the tyrosine residues within these ITIMs are phosphorylated (24, 25). To examine whether KIT activation induced CD72 phosphorylation or dephosphorylation in mast cells, and whether the phosphorylation status of CD72 was further modified after CD72 ligation, huMCs were stimulated for 5 min with SCF in the absence or presence of BU40 or rCD100. Cell lysates were then prepared, CD72 immunoprecipitated with an anti-CD72 Ab, and the immunoprecipitates probed for phosphotyrosine and the association of SHP-1. Lysates were also immunoprecipitated with a control Ab to assess nonspecific interactions. Using the control Ab for immunoprecipitating, we detected no increase in the tyrosine phosphorylation of CD72 or its association with SHP-1 under any of the experimental conditions described (data not shown).

Using the anti-CD72 Ab for immunoprecipitations, a slight, but detectable, constitutive tyrosine phosphorylation of CD72 was observed under resting conditions (Fig. 2*A*, 2*B*). This was associated with a similar slight, but detectable, constitutive association of SHP-1 with CD72 (Fig. 2*A*, 2*B*). Challenging the cells with SCF in the absence of BU40 or rCD100 induced minimal change in tyrosine phosphorylation of CD72 and no detectable increase in association of SHP-1 with CD72 (Fig. 2*A*). When the cells were challenged with SCF in the presence of BU40 or rCD100; however, there was an appreciable increase in tyrosine phosphorylation of CD72 that was linked to a marked enhancement of the association of SHP-1 with CD72 (Fig. 2*A*). However, when the cells were challenged with BU40 or rCD100 in the absence of SCF, we could not detect a significant change in the level of the phosphorylation of CD72 or the association between CD72 and SHP-1 (Fig. 2*B*).

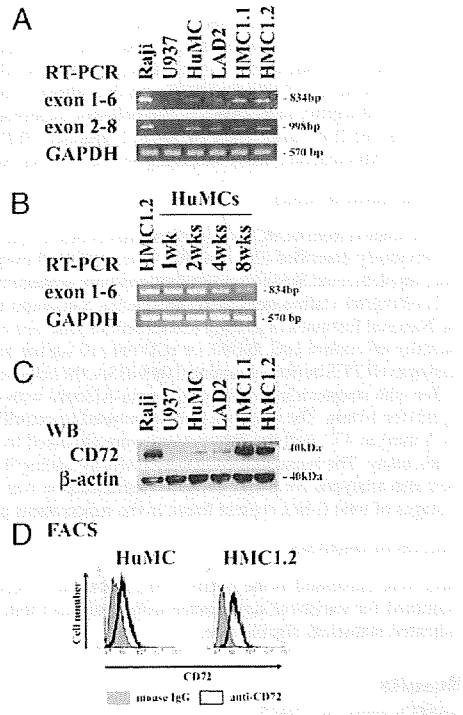

FIGURE 1. HuMCs and mast cell lines express CD72. *A*, RT-PCR. *B*, Western blotting. *C*, Flow cytometry were performed as described in *Materials and Methods*. The Raji cells were used as a positive control and the U937 cells as a negative control.

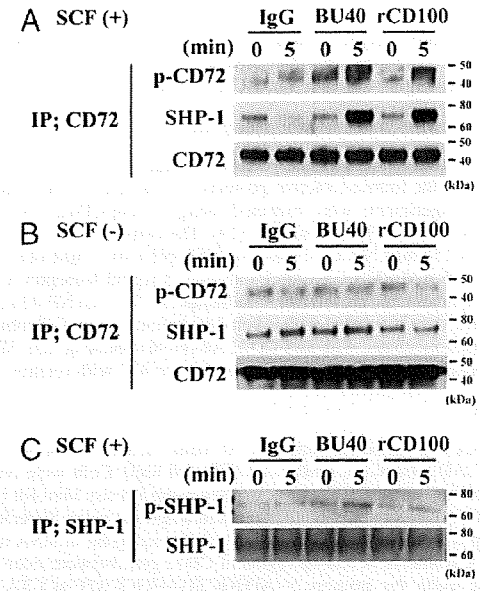

FIGURE 2. The effects of BU40 or rCD100 on the tyrosine phosphorylation of CD72, the association of SHP-1 with CD72 and the tyrosine phosphorylation of SHP-1 in huMCs. *A*, BU40 or rCD100 administration with SCF to huMCs induces the tyrosine phosphorylation of CD72 and the association with SHP-1, whereas (*B*) BU40 or rCD100 administration in the absence of SCF did not. HuMCs were incubated for 0 or 5 min with control IgG (10 μg/ml), BU40 (10 μg/ml), or rCD100 (10 μg/ml) in the presence or absence of SCF (10 ng/ml). CD72 was immunoprecipitated with anti-CD72 (H-96), and visualized with antiphosphotyrosine 4G10, anti–SHP-1, or anti-CD72. *C*, BU40 or rCD100 administration with SCF (10 ng/ml) to huMCs induces the tyrosine phosphorylation of SHP-1, when incubated for 5 min. SHP-1 was immunoprecipitated with an anti–SHP-1 Ab (C-19), and visualized with antiphosphotyrosine 4G10 or anti–SHP-1. Data are representative of three individual experiments.

Tyrosine phosphorylation of SHP-1 upregulates the phosphatase activity of SHP-1 (26). To assess whether ligation of CD72 induced tyrosine phosphorylation of SHP-1 in addition to recruitment, huMCs were stimulated with SCF concurrently with CD72 ligation, whole cell lysates were immunoprecipitated with an anti–SHP-1 Ab, then the immunoprecipitated proteins probed with an antiphosphotyrosine Ab. Slight tyrosine phosphorylation of SHP-1 was observed under resting conditions (Fig. 2*C*). However, when the cells were challenged with SCF in the presence of BU40 or rCD100, the tyrosine phosphorylated SHP-1 levels were observed to increase (Fig. 2*C*).

Taken together, these data provide support for the conclusion that concurrent ligation of CD72 and KIT results in the activation and recruitment of SHP-1 to CD72 with the potential to downregulate KIT-mediated responses in mast cells. We therefore next examined the effects of the CD72 agonistic Ab BU40 and rCD100 on KIT-mediated mast cell function.

CD72 ligation suppresses KIT-dependent growth of huMCs

To explore the potential ability of ligated CD72 to downregulate mast cell function, we next examined the effects of the agonistic Ab against human CD72, BU40, or rCD100, on indices of KIT-mediated growth of huMCs. To evaluate the potential role of CD72 in controlling progression through the cell cycle, cytokine-starved huMCs were cultured with SCF for 30 min with or without control IgG, BU40, or rCD100, then the cell cycle status of the cells was assessed by flow cytometry. The proportion of huMCs in G2/M and S phases after a 30-min exposure to SCF was not reduced by control Ab. However, administration of either BU40 or rCD100, together with SCF, resulted in a marked reduction in the ratio of cells in the G2/M and S phases of cell cycle, indicating arrested cell growth (Table I). To provide further support for this conclusion, we examined the abilities of BU40 and rCD100 to inhibit KIT-induced proliferation of huMCs as assessed by BrdU assay. HuMCs were cultured for 24 h in the absence or presence of SCF and control IgG, SCF and BU40, or SCF and rCD100, then the relative growth rates determined. As in the case with cell cycle arrest, both BU40 and rCD100 significantly reduced the growth of huMCs detected in the BrdU assay (Fig. 3*A*), providing further evidence that ligation of CD72 induces downregulation of KIT-mediated growth of huMCs.

CD72 ligation downregulates KIT-induced huMC chemotaxis and MCP-1 (CCL2) production

In addition to regulating cell growth, SCF-dependent KIT activation induces mast cell chemotaxis and the production of MCP-1 (CCL2) (2). We, thus, next investigated if these parameters were downregulated by CD72 ligation in a similar manner to that observed on cell growth. To evaluate the potential of CD72 to downregulate SCF-induced chemotaxis (27), cytokine-starved huMCs were placed in the upper chambers of dual chemotactic wells, then the cells were allowed to migrate to the lower chambers in response to SCF for 4 h in the absence and presence of control IgG, BU40, or rCD100. From Fig. 3*B*, it can be seen that both BU40 and rCD100 significantly reduced SCF-induced huMC chemotaxis, whereas the control IgG had little effect.

KIT activation promotes MCP-1 (CCL2) secretion from human lung mast cells even in the absence of FcεRI stimulation (22). We

Table I. *Ligation of CD72 with BU40 or rCD100 suppresses KIT-mediated cell cycle progression of huMCs*

Treatment	Cells in G2/M and S Phases (%)
SCF only	6.93 ± 0.58
SCF and control IgG	7.39 ± 0.85
SCF and BU40	3.07 ± 0.22*
SCF and rCD100	3.60 ± 0.44*

After overnight culture in cytokine-free medium, huMCs were cultured for 30 min in HEPES buffer containing 0.04% BSA (huMCs) with SCF, SCF and control IgG, SCF and BU40, or SCF and rCD100. The cells were stained with propidium iodine, and then analyzed using a FACScan flow cytometer.

*$p < 0.01$, when compared with the value of SCF and control IgG.

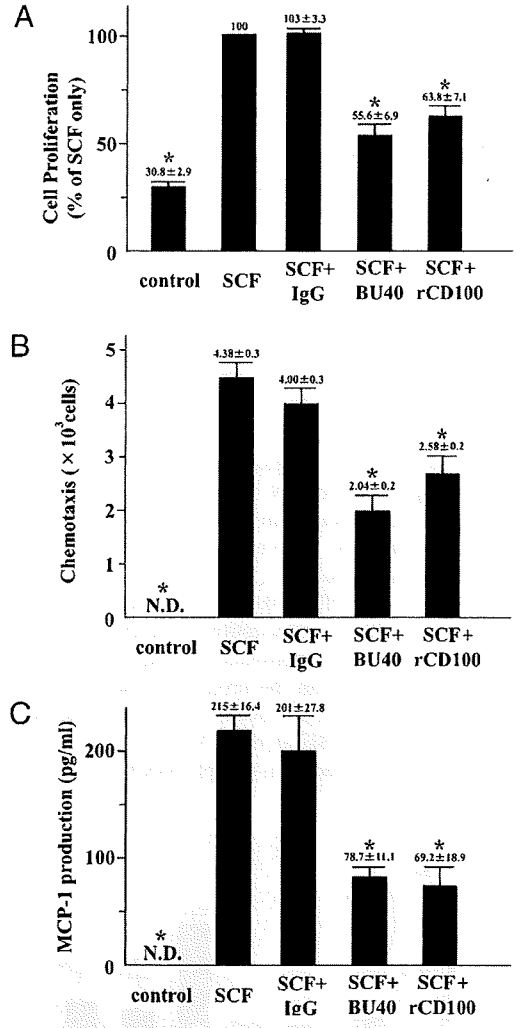

FIGURE 3. The effects of BU40 or rCD100 on KIT-mediated responses of huMCs. *A*, The ligation of CD72 with BU40 or rCD100 suppresses KIT-induced proliferation of huMCs (BrdU assay, $n = 4$). HuMCs were incubated for 24 h with or without control IgG, BU40, or rCD100 (10 μg/ml, respectively) in the absence or presence of SCF (10 ng/ml). HuMC proliferation was assessed using a BrdU cell proliferation assay kit according to the manufacture's protocol. The relative values are indicated when the value of SCF and control IgG is 100. *$p < 0.05$, when compared with SCF and control IgG. *B*, Ligation of CD72 with BU40 or rCD100 suppresses SCF-induced mast cell chemotaxis. HuMCs (1×10^5) with or without control IgG, BU40, or rCD100 (10 μg/ml, respectively) were incubated in the upper chambers to assess the migration to the lower chambers containing SCF (30 ng/ml) for 4 h ($n = 3$). After the incubation, cell migration to the lower wells was assed by counting by microscopy. *$p < 0.05$, when compared with SCF and control IgG. *C*, Ligation of CD72 with BU40 or rCD100 suppresses SCF-induced MCP-1 secretion. HuMCs were incubated for 6 h with or without control IgG, BU40, or rCD100 (10 μg/ml, respectively) in the absence or presence of SCF (10 ng/ml) ($n = 5$). The culture supernatants were used for the ELISA assay for human MCP-1. *$p < 0.05$, when compared with SCF and control IgG.

therefore next explored the ability of BU40 or rCD100 to inhibit SCF-induced MCP-1 secretion from huMCs. HuMCs were cultured in medium containing SCF in the absence or presence of control IgG, BU40, or rCD100 for 6 h, then the supernatants were assayed for MCP-1 content by ELISA. As with cell growth and chemotaxis, BU40 and rCD100 significantly inhibited SCF-mediated huMC MCP-1 production (Fig. 3*C*).

CD72 ligation does not affect FcεRI-mediated huMC degranulation but inhibits the augmentation of this response by KIT

Ag-mediated aggregation of high-affinity receptors for IgE (FcεRI) triggers degranulation of mast cells (1, 2). This response can be further augmented after SCF-dependent KIT activation (6, 8). We, thus, examined whether these responses were downregulated after CD72 ligation in huMCs. Concurrent ligation of CD72 with FcεRI failed to reduce the response observed with FcεRI alone. However, CD72 ligation resulted in a significant reduction in the augmentation of this response by SCF (Fig. 4), demonstrating that the KIT-mediated, but not FcεRI-mediated component of this response could be downregulated by CD72 ligation.

CD72 ligation induces downregulation of KIT-mediated phosphorylation of signaling molecules

SCF-induced KIT dimerization results in KIT autophosphorylation, thereby recruiting critical signaling molecules into the receptor signaling complex where they become phosphorylated, allowing their regulation of downstream processes required for mast cell growth and function (6). Such events include recruitment and activation of Src family kinases (SFKs) and downstream signaling cascades regulated by PI3K, MAPKs (MAPKs), and signal transducers and activators of transcription 3 (Stat3) (6). We therefore examined whether the recruitment of SHP-1, after ligation of CD72, was associated with the reversal of these signaling pathways. HuMCs were again stimulated with SCF in the presence or absence of control IgG, BU40, or rCD100 for 15 or 30 mins, then lysates probed for phospho-KIT, phospho-AKT (a surrogate marker for PI3K activation), phospho-SFKs (recognizes both phospho-Lyn and phospho-Fyn), phospho-ERK1/2 MAPKs, and phospho-Stat3.

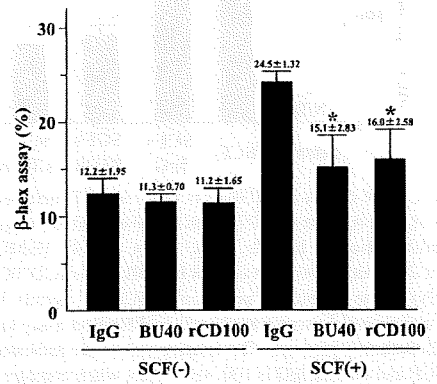

FIGURE 4. The effects of BU40 or rCD100 on IgE-triggered degranulation of huMCs. BU40 or rCD100 administration did not inhibit IgE/streptavidin-induced (FcεRI-mediated) degranulation in the absence of SCF. However, BU40 and rCD100 administration suppressed SCF-induced augmentation of IgE/streptavidin-induced degranulation of huMCs. Degranulation from huMCs was evaluated by β-hex release as described in *Materials and Methods*. HuMCs were sensitized overnight in cytokine-free medium containing biotinylated-human myeloma IgE (100 ng/ml) in the presence of control IgG, BU40, or rCD100 (10 μg/ml, respectively), and activated with streptavidin (100 ng/ml) with or without SCF (1 ng/ml) for 30 min ($n = 3$). $*p < 0.05$, when compared with control IgG in the absence or presence of SCF.

At both time points, it can be seen that phosphorylation of KIT, SFKs, and ERK1/2 was markedly reduced in the cells treated with BU40 and rCD100 (Fig. 5). However, there were no marked differences in the phosphorylation of either Stat3 (data not shown) or AKT (Fig. 5) after treatment of the cells with these reagents, though both proteins were phosphorylated by SCF challenge (data not shown). These data suggest that the ability of CD72 to inhibit mast cell growth and function is linked to the SHP-1–dependent downregulation of pathways regulating and regulated by SFKs and ERK1/2, but not by PI3K/AKT and Stat3.

CD72 downregulates the growth and the phosphorylation of signaling molecules in HMC1.2 cells

The HMC1.2 huMC line was established from a patient with mast cell leukemia (17). This cell line harbors gain-of-function mutations in KIT, thus proliferates independently of SCF (5, 18). We examined the effect of BU40 or rCD100 on mutated KIT-induced growth of HMC1.2 cells by cell cycle analysis and by BrdU assay, as for the huMC analysis. HMC1.2 cells were cultured without SCF for 30 min with or without control IgG, BU40, or rCD100, then the cell cycle status of the cells was assessed by flow cytometry. The proportion of HMC1.2 cells in G2/M and S phases after 30 min exposure to rCD100 or BU40 was not reduced compared to that observed with exposure to control IgG (none, 23.6 ± 1.38%; control IgG, 23.3 ± 1.78%; BU40, 20.9 ± 1.93%; rCD100, 21.5 ± 2.36%). We then assessed the effects of rCD100 or BU40 by BrdU assay. In contrast to the cell cycle data, rCD100 or BU40 markedly suppressed the HMC1.2 cell proliferation for 24 h by this assay (Fig. 6).

To address the negative effects of BU40 or rCD100 on HMC1.2 cells, we evaluated the phosphorylation status of CD72 and SHP-1 by immunoprecipitation, and of signal molecules by immunoblotting. Incubation of HMC1.2 cells with BU40 or rCD100 increased the tyrosine phosphorylation of CD72 and SHP-1 and the association between CD72 and SHP-1 even in the absence of SCF stimulation (Fig. 7*A*, 7*C*). In addition, we observed the suppressive effects of BU40 or rCD100 on the mutated KIT-induced phosphorylations of KIT, SFKs, and ERK (Fig. 7*D*). These data, which were compatible with the responses observed in the SCF-stimulated huMCs, show that the aberrant growth of the tumor cell line could also be inhibited on CD72 ligation.

Discussion

The ITIM-bearing inhibitory receptor, CD72, has been reported to be expressed on B cells, T cells, NK cells, dendritic cells, and

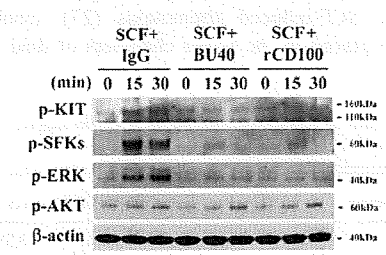

FIGURE 5. Ligation of CD72 with BU40 or rCD100 suppresses the activation of KIT signaling in huMCs. HuMCs were incubated for the indicated times with control IgG, BU40, or rCD100 (10 μg/ml, respectively) in the presence of SCF (10 ng/ml). The levels of phospho-KIT, phospho-ERK, phospho-Src family kinases (Tyr 416), and β-actin were then evaluated by immunoblot analysis. Data are representative from three individual experiments.

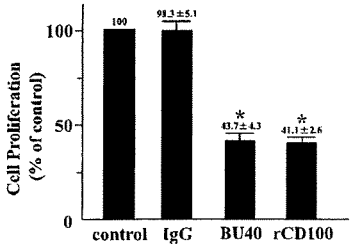

FIGURE 6. Ligation of CD72 with BU40 or rCD100 suppresses mutated KIT-driven proliferation of HMC1.2 (BrdU assay, $n = 3$). HMC1.2 cells were incubated for 24 h with control medium, control IgG, BU40, or rCD100 (10 μg/ml, respectively). Incorporation of BrdU into the HMC1.2 cells was assessed using a BrdU cell proliferation assay kit according to the manufacture's protocol. The relative values are indicated when the value of control IgG is 100. $*p < 0.05$, when compared with control IgG.

macrophages (13, 28). In this study, we now demonstrate that CD72 is also expressed on huMCs derived from CD34-positive peripheral blood and on huMC lines. This was demonstrated through the presence of mRNA for CD72, and by CD72 protein expression as detected by Western blot and by FACS analysis (Fig. 1*A–C*). mRNA for CD72 was observed at all stages of development of the huMC cultures examined. However, there was a trend for reduced message in the more mature cultures. Thus, in mature mast cells (8 wk culture), CD72 protein expression was substantially lower than in the HMC 1.2 cells. Regardless, the surface expression as detected by FACS was comparable. A possible explanation for this is that, in HMC1.2 cells, the protein is partly retained in the cytosol (data not shown) due to defective regulation of translocation of CD72 protein to the cell surface after transcription. Differences in CD72 protein expression between the huMCs and HMC1.2 cells may be reflective of the transformed nature of the latter cell type or may reflect an immature phenotype of the transformed cells.

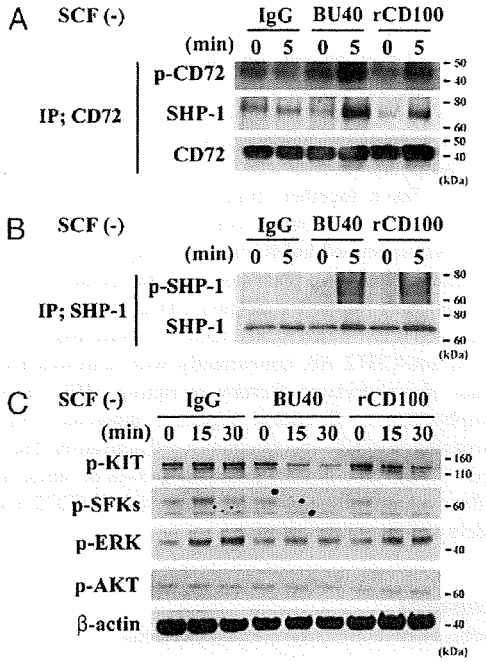

FIGURE 7. The effects of BU40 or rCD100 on the tyrosine phosphorylation of CD72, the association with SHP-1 with CD72, and on the activation of signaling molecules in HMC1.2 cells. BU40 or rCD100 administration to HMC1.2 cells upregulates (*A*) the tyrosine phosphorylation of CD72, the association with SHP-1, and (*B*) the tyrosine phosphorylation of SHP-1. HMC1.2 cells were incubated for 0 or 5 min with control IgG, BU40, or rCD100 (10 μg/ml, respectively) in the absence of SCF. CD72 was immunoprecipitated with anti-CD72 (H-96) or anti–SHP-1 (C-19), and visualized with antiphosphotyrosine 4G10, anti–SHP-1, or anti-CD72. Data are representative from three individual experiments. *C*, Ligation of CD72 with BU40 or rCD100 suppresses the activation of signal molecules in HMC1.2 cells. HMC1.2 cells were incubated for the indicated time with control IgG, BU40, or rCD100 (10 μg/ml, respectively). The levels of phospho-KIT, phospho-ERK, phospho-Src family kinases (Tyr 416), and β-actin were then asssed by immunoblot analysis. Data are representative from three individual experiments.

Our data do differ from a previous study where the expression of CD72 by FACS analysis was not detected on huMCs derived from umbilical cord blood (29). However, in that report, the expression of MAFA, which is known to be expressed in mast cells (9), was also not detected. The difference in CD72 expression between the two reports may thus reflect different sensitivities of the Abs used or difference of the origins of the mast cell progenitors. Nevertheless, based on the data presented in this study, CD72 can now be added to the list of inhibitory receptors that are documented to be expressed in mast cells.

The natural ligand for CD72 is recognized to be CD100, thus, an advantage of using CD72 to downregulate SCF-dependent mast cell function is that this can be achieved through interaction of CD72 with its natural ligand. Indeed, in this study, we observed that the cellular responses induced by an anti-CD72 Ab could be mimicked by CD100. Expression of CD100 is reported in B cells, T cells, and neuronal cells (30), but to date has not been reported in mast cells. Our preliminary studies have also failed to detect CD100 expression in primary cultured huMCs and in the HMC1.2 huMC line (data not shown). Regardless, it is possible that interaction between CD72-expressing mast cells and CD100-expressing immune cells may influence mast cell function, as is the case with the interaction among CD72-expressing B cells and CD100-expressing T cells (30). Associations between mast cells and neurons have also been reported (31). Thus, such events may also influence mast cell function via CD72–CD100 interactions. Certainly, our data do provide supportive evidence that ligation of CD72 by CD100, or by means of an agonistic Ab, has the potential to modify KIT-mediated mast cell responses. In this respect, we observed that both rCD100 and an agonistic anti-CD72 Ab downregulated the KIT-dependent growth of huMCs (Fig. 3*A*), in addition to significantly reducing SCF-induced huMC chemotaxis, SCF-induced MCP-1 (CCL2) production (Fig. 3*B*, 3*C*), and the SCF-enhancement of IgE-dependent degranulation (Fig. 4).

Cellular responses regulated by CD72 have been primarily investigated in B cells and B cell lines (13). However, these studies have sometimes produced conflicting data (13). Although the consensus of studies report that CD72 ligation positively regulates responses in

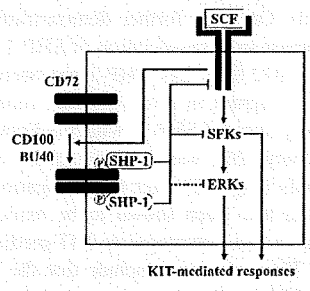

FIGURE 8. Proposed model of the effects of CD72–CD100 system on huMCs.

B cells by reversing the inhibitory potential of CD72 (14, 32–39), other studies have revealed that CD72 ligation further increases its inhibitory potential (40). Specifically, CD72 ligation has been reported to induce the proliferation of B cells (32, 33), and to positively regulate CD40-induced (14) and Ag-mediated (36) proliferation of B cells. Furthermore, CD72 ligation by an anti-CD72 Ab was reported to rescue B cell apoptosis mediated by BCR ligation and IgM hypercrosslinking (38, 40). In contrast to these data, which imply that CD72 ligation reverses its inhibitory potential, CD72 expression in B cell line K46 μmλ and incubation of splenic B cells with an anti-CD72 Ab resulted in downmodulation of BCR-mediated ERK activation and calcium mobilization (40). These data imply that CD72 ligation promotes its inhibitory potential.

These apparently conflicting data have led to the conclusion that CD72 may regulate positive and negative signaling pathways for the regulation of B cell responses and that this may, in part, be related to the stages of B cell development (13). Regardless, the ability of CD72 to regulate cellular responses is dependent on its phosphorylation status, hence its ability to recruit SHP-1, an interaction that is reported to be negatively influenced through its interaction with CD72-bound Grb2 (41). It has been proposed that, in the scenario in which CD72 ligation reverses its inhibitory activity, rCD100 or the agonistic Ab results in dissociation of CD72 from the B cell signaling complex thus reversing BCR-dependent phosphorylation of CD72. In contrast, in the scenario, in which CD72 ligation induces its inhibitory activity, the agonistic anti-CD72 Ab promotes association of CD72 with the receptor signaling-complex thus allowing its phosphorylation and recruitment of SHP-1 (40).

In resting B cells, there appears to be minimal constitutive phosphorylation of CD72 (25). However, in the huMCs, we observed that there was a slight but detectible constitutive phosphorylation of CD72 and its association with SHP-1 in the resting state (Fig. 2). Hence, the possibility exists that CD72 may help regulate the basal activation state of the huMCs. Our data, furthermore, demonstrate that in these cells, ligation of CD72 with either rCD100 or the agonistic Ab BU40 concurrently with KIT activation, results in the activation of necessary events that allow CD72 to inhibit KIT-mediated signaling. Thus, in the case of mast cells, the mode of the responses elicited by rCD100 and BU40 would appear similar to that reported in the splenic B cells (40), which is suggestive of permissive phosphorylation of CD72 by KIT after CD72 ligation. This conclusion was further supported by the enhancement of tyrosine phosphorylation of CD72 observed in the CD72-immunoprecipitates from mast cells incubated with BU40 or rCD100 and triggered through KIT (Fig. 2*A*, 2*B*).

Unlike the BCR, KIT possesses inherent catalytic activity that is increased on SCF-induced KIT dimerization. An increase in CD72 phosphorylation was not observed in cells incubated with rCD100 or BU40 in the absence of KIT activation (Fig. 2*B*). It is likely that the inducible phosphorylation of CD72 observed in the huMCs is directly due to phosphorylation by KIT, contrary to the case in immature B cells. Our data further demonstrated that there was a significant increase in the association of SHP-1 with the tyrosine phosphorylated CD72 (Fig. 2*A*). SHP-1 has been demonstrated to downregulate KIT signals in vivo (42) and, indeed, we observed that the phosphorylation of SHP-1, which is known to increase its phosphatase activity (26), was elevated in the huMCs (Fig. 2*C*) and HMC1.2 cells (Fig. 7*B*) after CD72 ligation. In addition to CD72, SHP-1 has also been shown to be associated with other inhibitory receptors that downregulate KIT-mediated responses in mast cells (12). Thus, we can conclude that the ability of ligated CD72 to inhibit KIT-mediated responses in mast cells is linked to its ability to recruit SHP-1 after its phophorylation.

SHP-1 dephosphorylates regulatory tyrosine residues on critical proteins that participate in signaling cascades initiated by multiple receptors, including KIT (6). We observed that CD72 phosphorylation led to the suppression of the phosphorylation of KIT, SFKs, and ERK induced by SCF challenge (Fig. 5), but not of AKT or Stat3. Both KIT and SFKs are known to be directly dephosphorylated by interactions with SHP-1 (43–45). Therefore, it is likely that the downregulated phosphorylation of KIT and SFKs induced by costmulation of KIT with CD72 in mast cells was a consequence of the formation of the CD72–SHP-1 complex. It is unclear whether SHP-1 can directly regulate the activation of ERK (46, 47). Therefore, there are two possible explanations for the ERK dephosphorylation observed in the huMCs in response to coactivation of KIT and CD72: 1) The suppressed activation of ERK by CD72 stimulation was mediated directly by the CD72–SHP-1 complex or 2) the suppressed ERK phosphorylation was indirect due to the downregulation of SFKs activity, as ERK phosphorylation is known to be regulated by SFKs (48).

Regardless of whether direct or indirect, the downregulation of the KIT-dependent phosphorylation of KIT, SFKs, and ERK by the interaction of SHP-1 with phosphorylated CD72 would certainly account for the ability of ligated CD72 to downregulate KIT-mediated responses in huMCs. In this respect, in mast cells, the SFKs, Lyn and Fyn, play important roles in KIT-mediated proliferation and chemotaxis (49) and ERK participates in the process of KIT-mediated proliferation and MCP-1 production (50). The downregulation of SCF-induced phosphorylation of SFKs by CD72 would also account for the observed inhibition of SCF-enhanced degraulation after CD72 ligation (Fig. 4). The inability of ligated CD72 to decrease the degranulation response induced by FcεRI aggregation alone again points to the requirement of direct phosphorylation of CD72 by KIT to induced inhibitory responses. Taken together, from the previously described conclusions, we can now put together a model of how CD72 may regulate KIT-mediated huMC function (Fig. 8).

In summary, we have presented data that demonstrates that the ITIM-containing inhibitory receptor CD72 is expressed in huMCs and mast cell lines. When ligated either by its natural ligand CD100 or by an anti-CD72 Ab, concurrently with activated KIT, CD72 becomes phosphorylated thereby recruiting SHP-1 resulting in dephosphorylation of critical signaling molecules resulting in downregulation of KIT-mediated mast cell activation. The ability of ligated CD72 to also downregulate the growth of tumor mast cells provides evidence of the potential application of CD72 in mast cell disorders such as mastocytosis.

Disclosures

The authors have no financial conflicts of interest.

References

1. Kraft, S., and J. P. Kinet. 2007. New developments in FcεRI regulation, function and inhibition. *Nat. Rev. Immunol.* 7: 365–378.
2. Okayama, Y., and T. Kawakami. 2006. Development, migration, and survival of mast cells. *Immunol. Res.* 34: 97–115.
3. Metcalfe, D. D. 2008. Mast cells and mastocytosis. *Blood* 112: 946–956.
4. Nagata, H., A. S. Worobec, C. K. Oh, B. A. Chowdhury, S. Tannenbaum, Y. Suzuki, and D. D. Metcalfe. 1995. Identification of a point mutation in the catalytic domain of the protooncogene c-kit in peripheral blood mononuclear cells of patients who have mastocytosis with an associated hematologic disorder. *Proc. Natl. Acad. Sci. USA* 92: 10560–10564.
5. Furitsu, T., T. Tsujimura, T. Tono, H. Ikeda, H. Kitayama, U. Koshimizu, H. Sugahara, J. H. Butterfield, L. K. Ashman, Y. Kanayama, et al. 1993. Identification of mutations in the coding sequence of the proto-oncogene c-kit in a human mast cell leukemia cell line causing ligand-independent activation of c-kit product. *J. Clin. Invest.* 92: 1736–1744.
6. Gilfillan, A. M., and C. Tkaczyk. 2006. Integrated signalling pathways for mast-cell activation. *Nat. Rev. Immunol.* 6: 218–230.

7. Jensen, B. M., C. Akin, and A. M. Gilfillan. 2008. Pharmacological targeting of the KIT growth factor receptor: a therapeutic consideration for mast cell disorders. *Br. J. Pharmacol.* 154: 1572–1582.
8. Gilfillan, A. M., R. D. Peavy, and D. D. Metcalfe. 2009. Amplification mechanisms for the enhancement of antigen-mediated mast cell activation. *Immunol. Res.* 43: 15–24.
9. Li, L., and Z. Yao. 2004. Mast cell and immune inhibitory receptors. *Cell. Mol. Immunol.* 1: 408–415.
10. Cherwinski, H. M., C. A. Murphy, B. L. Joyce, M. E. Bigler, Y. S. Song, S. M. Zurawski, M. M. Moshrefi, D. M. Gorman, K. L. Miller, S. Zhang, et al. 2005. The CD200 receptor is a novel and potent regulator of murine and human mast cell function. *J. Immunol.* 174: 1348–1356.
11. Bachelet, I., A. Munitz, B. Berent-Maoz, D. Mankuta, and F. Levi-Schaffer. 2008. Suppression of normal and malignant kit signaling by a bispecific antibody linking kit with CD300a. *J. Immunol.* 180: 6064–6069.
12. Unkeless, J. C., and J. Jin. 1997. Inhibitory receptors, ITIM sequences and phosphatases. *Curr. Opin. Immunol.* 9: 338–343.
13. Wu, H. J., and S. Bondada. 2009. CD72, a coreceptor with both positive and negative effects on B lymphocyte development and function. *J. Clin. Immunol.* 29: 12–21.
14. Kumanogoh, A., C. Watanabe, I. Lee, X. Wang, W. Shi, H. Araki, H. Hirata, K. Iwahori, J. Uchida, T. Yasui, et al. 2000. Identification of CD72 as a lymphocyte receptor for the class IV semaphorin CD100: a novel mechanism for regulating B cell signaling. *Immunity* 13: 621–631.
15. Kirshenbaum, A. S., J. P. Goff, T. Semere, B. Foster, L. M. Scott, and D. D. Metcalfe. 1999. Demonstration that human mast cells arise from a progenitor cell population that is CD34(+), c-kit(+), and expresses aminopeptidase N (CD13). *Blood* 94: 2333–2342.
16. Kirshenbaum, A. S., C. Akin, Y. Wu, M. Rottem, J. P. Goff, M. A. Beaven, V. K. Rao, and D. D. Metcalfe. 2003. Characterization of novel stem cell factor responsive human mast cell lines LAD 1 and 2 established from a patient with mast cell sarcoma/leukemia; activation following aggregation of FcεRI or FcγRI. *Leuk. Res.* 27: 677–682.
17. Butterfield, J. H., D. Weiler, G. Dewald, and G. J. Gleich. 1988. Establishment of an immature mast cell line from a patient with mast cell leukemia. *Leuk. Res.* 12: 345–355.
18. Sundström, M., H. Vliagoftis, P. Karlberg, J. H. Butterfield, K. Nilsson, D. D. Metcalfe, and G. Nilsson. 2003. Functional and phenotypic studies of two variants of a human mast cell line with a distinct set of mutations in the c-kit proto-oncogene. *Immunology* 108: 89–97.
19. Ishida, I., A. Kumanogoh, K. Suzuki, S. Akahani, K. Noda, and H. Kikutani. 2003. Involvement of CD100, a lymphocyte semaphorin, in the activation of the human immune system via CD72: implications for the regulation of immune and inflammatory responses. *Int. Immunol.* 15: 1027–1034.
20. Kim, M. S., H. S. Kuehn, D. D. Metcalfe, and A. M. Gilfillan. 2008. Activation and function of the mTORC1 pathway in mast cells. *J. Immunol.* 180: 4586–4595.
21. Kataoka, T. R., and Y. Nishizawa. 2008. Stat4 suppresses the proliferation of connective tissue-type mast cells. *Lab. Invest.* 88: 856–864.
22. Baghestanian, M., R. Hofbauer, H. P. Kiener, H. C. Bankl, F. Wimazal, M. Willheim, O. Scheiner, W. Füreder, M. R. Müller, D. Bevec, et al. 1997. The c-kit ligand stem cell factor and anti-IgE promote expression of monocyte chemoattractant protein-1 in human lung mast cells. *Blood* 90: 4438–4449.
23. Schwarting, R., R. Castello, G. Moldenhauer, A. Pezzutto, I. von Hoegen, W. D. Ludwig, J. R. Parnes, and B. Dörken. 1992. Human Lyb-2 homolog CD72 is a marker for progenitor B-cell leukemias. *Am. J. Hematol.* 41: 151–158.
24. Adachi, T., H. Flaswinkel, H. Yakura, M. Reth, and T. Tsubata. 1998. The B cell surface protein CD72 recruits the tyrosine phosphatase SHP-1 upon tyrosine phosphorylation. *J. Immunol.* 160: 4662–4665.
25. Wu, Y., M. J. Nadler, L. A. Brennan, G. D. Gish, J. F. Timms, N. Fusaki, J. Jongstra-Bilen, N. Tada, T. Pawson, J. Wither, et al. 1998. The B-cell transmembrane protein CD72 binds to and is an in vivo substrate of the protein tyrosine phosphatase SHP-1. *Curr. Biol.* 8: 1009–1017.
26. Zhang, Z., K. Shen, W. Lu, and P. A. Cole. 2003. The role of C-terminal tyrosine phosphorylation in the regulation of SHP-1 explored via expressed protein ligation. *J. Biol. Chem.* 278: 4668–4674.
27. Nilsson, G., J. H. Butterfield, K. Nilsson, and A. Siegbahn. 1994. Stem cell factor is a chemotactic factor for human mast cells. *J. Immunol.* 153: 3717–3723.
28. Alcón, V. L., C. Luther, D. Balce, and F. Takei. 2009. B-cell co-receptor CD72 is expressed on NK cells and inhibits IFN-γ production but not cytotoxicity. *Eur. J. Immunol.* 39: 826–832.
29. Kepley, C. L., S. Taghavi, G. Mackay, D. Zhu, P. A. Morel, K. Zhang, J. J. Ryan, L. S. Satin, M. Zhang, P. P. Pandolfi, and A. Saxon. 2004. Co-aggregation of FcγRII with FcεRI on human mast cells inhibits antigen-induced secretion and involves SHIP-Grb2-Dok complexes. *J. Biol. Chem.* 279: 35139–35149.
30. Kumanogoh, A., and H. Kikutani. 2001. The CD100-CD72 interaction: a novel mechanism of immune regulation. *Trends Immunol.* 22: 670–676.
31. Ito, A., M. Hagiyama, and J. Oonuma. 2008. Nerve-mast cell and smooth muscle-mast cell interaction mediated by cell adhesion molecule-1, CADM1. *J. Smooth Muscle Res.* 44: 83–93.
32. Subbarao, B., and D. E. Mosier. 1983. Induction of B lymphocyte proliferation by monoclonal anti-Lyb 2 antibody. *J. Immunol.* 130: 2033–2037.
33. Subbarao, B., and D. E. Mosier. 1984. Activation of B lymphocytes by monovalent anti-Lyb-2 antibodies. *J. Exp. Med.* 159: 1796–1801.
34. Snow, E. C., J. J. Mond, and B. Subbarao. 1986. Enhancement by monoclonal anti-Lyb-2 antibody of antigen-specific B lymphocyte expansion stimulated by TNP-Ficoll and T lymphocyte-derived factors. *J. Immunol.* 137: 1793–1796.
35. Pan, C., N. Baumgarth, and J. R. Parnes. 1999. CD72-deficient mice reveal nonredundant roles of CD72 in B cell development and activation. *Immunity* 11: 495–506.
36. Li, D. H., J. W. Tung, I. H. Tarner, A. L. Snow, T. Yukinari, R. Ngernmaneepothong, O. M. Martinez, and J. R. Parnes. 2006. CD72 downmodulates BCR-induced signal transduction and diminishes survival in primary mature B lymphocytes. *J. Immunol.* 176: 5321–5328.
37. Wu, H. J., C. Venkataraman, S. Estus, C. Dong, R. J. Davis, R. A. Flavell, and S. Bondada. 2001. Positive signaling through CD72 induces mitogen-activated protein kinase activation and synergizes with B cell receptor signals to induce X-linked immunodeficiency B cell proliferation. *J. Immunol.* 167: 1263–1273.
38. Nomura, T., H. Han, M. C. Howard, H. Yagita, H. Yakura, T. Honjo, and T. Tsubata. 1996. Antigen receptor-mediated B cell death is blocked by signaling via CD72 or treatment with dextran sulfate and is defective in autoimmunity-prone mice. *Int. Immunol.* 8: 867–875.
39. Shi, W., A. Kumanogoh, C. Watanabe, J. Uchida, X. Wang, T. Yasui, K. Yukawa, M. Ikawa, M. Okabe, J. R. Parnes, et al. 2000. The class IV semaphorin CD100 plays nonredundant roles in the immune system: defective B and T cell activation in CD100-deficient mice. *Immunity* 13: 633–642.
40. Adachi, T., C. Wakabayashi, T. Nakayama, H. Yakura, and T. Tsubata. 2000. CD72 negatively regulates signaling through the antigen receptor of B cells. *J. Immunol.* 164: 1223–1229.
41. Baba, T., N. Fusaki, A. Aoyama, D. H. Li, R. M. Okamura, J. R. Parnes, and N. Hozumi. 2005. Dual regulation of BCR-mediated growth inhibition signaling by CD72. *Eur. J. Immunol.* 35: 1634–1642.
42. Paulson, R. F., S. Vesely, K. A. Siminovitch, and A. Bernstein. 1996. Signalling by the W/Kit tyrosine kinase is negatively regulated in vivo by the tyrosine phosphatase Shp1. *Nat. Genet.* 13: 309–315.
43. Rivera, J., and A. Olivera. 2007. Src family kinases and lipid mediators in control of allergic inflammation. *Immunol. Rev.* 217: 255–268.
44. Hibbs, M. L., and K. W. Harder. 2006. The duplicitous nature of the Lyn tyrosine kinase in growth factor signaling. *Growth Factors* 24: 137–149.
45. Kozlowski, M., L. Larose, F. Lee, D. M. Le, R. Rottapel, and K. A. Siminovitch. 1998. SHP-1 binds and negatively modulates the c-Kit receptor by interaction with tyrosine 569 in the c-Kit juxtamembrane domain. *Mol. Cell. Biol.* 18: 2089–2099.
46. Xie, Z. H., J. Zhang, and R. P. Siraganian. 2000. Positive regulation of c-Jun N-terminal kinase and TNF-α production but not histamine release by SHP-1 in RBL-2H3 mast cells. *J. Immunol.* 164: 1521–1528.
47. You, M., and Z. Zhao. 1997. Positive effects of SH2 domain-containing tyrosine phosphatase SHP-1 on epidermal growth factor- and interferon-γ-stimulated activation of STAT transcription factors in HeLa cells. *J. Biol. Chem.* 272: 23376–23381.
48. Ueda, S., M. Mizuki, H. Ikeda, T. Tsujimura, I. Matsumura, K. Nakano, H. Daino, Z. Honda Zi, J. Sonoyama, H. Shibayama, et al. 2002. Critical roles of c-Kit tyrosine residues 567 and 719 in stem cell factor-induced chemotaxis: contribution of src family kinase and PI3-kinase on calcium mobilization and cell migration. *Blood* 99: 3342–3349.
49. O'Laughlin-Bunner, B., N. Radosevic, M. L. Taylor, C. Shivakrupa, C. DeBerry, D. D. Metcalfe, M. Zhou, C. Lowell, and D. Linnekin. 2001. Lyn is required for normal stem cell factor-induced proliferation and chemotaxis of primary hematopoietic cells. *Blood* 98: 343–350.
50. Wong, C. K., C. M. Tsang, W. K. Ip, and C. W. Lam. 2006. Molecular mechanisms for the release of chemokines from human leukemic mast cell line (HMC)-1 cells activated by SCF and TNF-α: roles of ERK, p38 MAPK, and NF-kappaB. *Allergy* 61: 289–297.

The Journal of Immunology

Roles of Sema4D Plexin-B1 Interactions in the Central Nervous System for Pathogenesis of Experimental Autoimmune Encephalomyelitis

Tatsusada Okuno, Yuji Nakatsuji, Masayuki Moriya, Hyota Takamatsu, Satoshi Nojima, Noriko Takegahara, Toshihiko Toyofuku, Yukinobu Nakagawa, Sujin Kang, Roland H. Friedel, Saburo Sakoda, Hitoshi Kikutani and Atsushi Kumanogoh

J. Immunol. 2010;184;1499-1506; originally published online Dec 28, 2009;
doi:10.4049/jimmunol.0903302
http://www.jimmunol.org/cgi/content/full/184/3/1499

The Journal of Immunology is published twice each month by The American Association of Immunologists, Inc., 9650 Rockville Pike, Bethesda, MD 20814-3994.

Print ISSN: 0022-1767 Online ISSN: 1550-6606.

Roles of Sema4D–Plexin-B1 Interactions in the Central Nervous System for Pathogenesis of Experimental Autoimmune Encephalomyelitis

Tatsusada Okuno,*,†,‡ Yuji Nakatsuji,‡ Masayuki Moriya,‡ Hyota Takamatsu,*,† Satoshi Nojima,*,† Noriko Takegahara,*,† Toshihiko Toyofuku,*,† Yukinobu Nakagawa,*,† Sujin Kang,*,† Roland H. Friedel,§,1 Saburo Sakoda,‡ Hitoshi Kikutani,¶ and Atsushi Kumanogoh*,†

Although semaphorins were originally identified as axonal guidance molecules during neuronal development, it is emerging that several semaphorins play crucial roles in various phases of immune responses. Sema4D/CD100, a class IV semaphorin, has been shown to be involved in the nervous and immune systems through its receptors plexin-B1 and CD72, respectively. However, the involvement of Sema4D in neuroinflammation still remains unclear. We found that Sema4D promoted inducible NO synthase expression by primary mouse microglia, the effects of which were abolished in plexin-B1–deficient but not in CD72-deficient microglia. In addition, during the development of experimental autoimmune encephalomyelitis (EAE), which was induced by immunization with myelin oligodendrocyte glycoprotein-derived peptides, we observed that the expression of Sema4D and plexin-B1 was induced in infiltrating mononuclear cells and microglia, respectively. Consistent with these expression profiles, when myelin oligodendrocyte glycoprotein-specific T cells derived from wild-type mice were adoptively transferred into plexin-B1–deficient mice or bone marrow chimera mice with plexin-B1–deficient CNS resident cells, the development of EAE was considerably attenuated. Furthermore, blocking Abs against Sema4D significantly inhibited neuroinflammation during EAE development. Collectively, our findings demonstrate the role of Sema4D–plexin-B1 interactions in the activation of microglia and provide their pathologic significance in neuroinflammation. *The Journal of Immunology*, **2010, 184: 1499–1506.**

Microglia, resident immune effector cells in the CNS, are thought to play a key role in the regulation of neuroinflammation (1). Although activated microglia are known to exert a beneficial role in host defense and tissue repair in the CNS, it has been suggested that they also participate in propagation of inflammation in the CNS through Ag presentation, production of proinflammatory cytokines or chemokines, and NO (2–4). In fact, the mechanisms of how activation of microglia is regulated have been extensively studied. For example, CD40, a member of the TNF receptor family, has been reported to be involved in microglial activation (5, 6). Interactions of CD40 with its ligand (CD154), which is primarily expressed by activated T cells, promote the activation of microglia in the context of enhanced expression of costimulatory molecules and production of proinflammatory cytokines or chemokines and NO (5). Therefore, CD40–CD40 ligand interactions have been implicated in various neurologic disorders such as multiple sclerosis, Alzheimer's disease, and Parkinson's disease (5, 7, 8). However, answers are elusive regarding how the immunoregulatory molecules are involved in neuroinflammation.

Sema4D/CD100 is a transmembrane-type semaphorin belonging to the class IV semaphorin subclass. Although semaphorins were initially identified as axonal guidance cues during neuronal development (9, 10), accumulating evidence now indicates that several semaphorins play a crucial role in physiologic and pathologic immune responses (11). The expression of Sema4D is abundantly observed in T cells, but only weakly detected in naive B cells, macrophages, and dendritic cells (DCs); however, its expression is significantly upregulated on cellular activation (12, 13). Regarding its receptor systems, Sema4D has been shown to use two distinct receptors, plexin-B1 in the nervous system and CD72 in the immune system (11, 14, 15). We previously demonstrated the activation of B cells and DCs through the Sema4D–CD72 interactions (15, 16); Sema4D-deficient mice display severe impairments in activation of B cells and DCs, resulting in impaired Ab production and Ag-specific T cell priming (13, 16). In the nervous system, Sema4D participates in axon guidance by regulating activities of RhoA

*Department of Immunopathology, ¶Department of Molecular Immunology, Research Institute for Microbial Diseases, †World Premier International Immunology Frontier Research Center, and ‡Department of Neurology, Osaka University Graduate School of Medicine, Osaka University, Osaka, Japan; and §Institute of Developmental Genetics, Helmholtz Center Munich, Neuherberg, Germany

[1]Current address: Department of Developmental and Regenerative Biology, Mount Sinai School of Medicine, New York, NY.

Received for publication October 13, 2009. Accepted for publication November 14, 2009.

This work was supported by research grants from the Ministry of Education, Culture, Sports, Science and Technology of Japan; Health and Labour Sciences Research Grants for research on intractable diseases from the Ministry of Health, Labor, and Welfare; the program for Promotion of Fundamental Studies in Health Sciences of the National Institute of Biomedical Innovation (to A.K., Y.N., and S.S.); the Target Protein Research Program of the Japan Science and Technology Agency (to T.T. and A.K.); the Uehara Memorial Foundation (to A.K.); and the Takeda Scientific Foundation (to T.T. and A.K.).

Address correspondence and reprint requests to Atsushi Kumanogoh, Department of Immunopathology, Research Institute for Microbial Diseases, Osaka University, 3-1 Yamada-oka, Suita, Osaka 565-0871, Japan, or Yuji Nakatsuji, Department of Neurology (D4), Osaka University Graduate School of Medicine, 2-2 Yamada-oka, Suita, Osaka 565-0871, Japan. E-mail addresses: kumanogo@ragtime.biken.osaka-u.ac.jp or yuji@neurol.med.osaka-u.ac.jp

The online version of this article contains supplemental material.

Abbreviations used in this paper: BM, bone marrow; DC, dendritic cell; EAE, experimental autoimmune encephalomyelitis; iNOS, inducible NO synthase; MG, primary microglia; MOG, myelin oligodendrocyte glycoprotein; PLP, proteolipid protein; SB, SB203580; SP, SP600125; St, standards.

www.jimmunol.org/cgi/doi/10.4049/jimmunol.0903302

through PDZ-ρ guanine nucleotide exchange factors and leukemia-associated RhoGEF (17). In addition, plexin-B1 has been shown to mediate repellent signals in hypocampal neurons by directly binding Rnd1 and downregulating R-ras activity in response to Sema4D (18). Collectively, these findings indicate the importance of Sema4D in both nervous and immune systems.

Regarding neuroinflammation, in which the immune system interacts with the nervous system, it has been suggested that semaphorins are pathogenetically significant. Sema7A expressed in T cells regulates inflammation of experimental autoimmune encephalomyelitis (EAE) (19, 20). In addition, it has been reported that Sema4D is relevant to HTLV-1–associated myelopathy (21). The expression of Sema4D was increased in the cerebrospinal fluid and spinal cords of patients with HTLV-1–associated myelopathy, in which T cell-derived Sema4D impaired immature oligodendrocytes (21). In addition, we previously reported that Sema4D-deficient mice were resistant to the development of EAE because of the impaired Ag-specific T cell priming in the draining lymph nodes (16). Although these facts suggest the relevance of Sema4D in neuroinflammatory diseases, it has not been fully elucidated how and to what extent Sema4D is involved in neuroinflammation.

In this study, we demonstrate enhanced activation of microglia through Sema4D–plexin-B1 interactions. In addition, we find that either plexin-B1–deficient mice or bone marrow (BM) chimera mice with CNS-specific plexin-B1 deficiency were resistant to the development of EAE after adoptive transfer of myelin oligodendrocyte glycoprotein (MOG)-specific T cells. We further present that the treatment with an Ab against Sema4D was effective for EAE blocking, including in the effector phase. These findings demonstrate the significance of Sema4D–plexin-B1 interactions in the inflamed CNS and provide a novel therapeutic target for neuroinflammatory diseases.

Materials and Methods

Mice

Sema4D- and plexin-B1–deficient on the C57BL/6 background were generated and maintained as described previously (13, 22, 23). CD72-deficient mice were provided by Dr. Parnes (Stanford University, Stanford, CA) (24). C57BL/6 (CD45.2 and CD45.1) and SJL mice were purchased from Nippon Clea (Hamamatsu, Japan) and Nippon Charles River (Kanagawa, Japan), respectively. All mice used in this study were maintained in a specific pathogen-free environment. All animal experimental procedures were consistent with our institutional guidelines.

Reagents for cell cultures

Agonistic anti-CD40 Ab (HM40-3), and recombinant mouse interferon-γ (IFN-γ) were purchased from BD Biosciences (San Diego, CA), and Genzyme-Techne (Cambridge, MA), respectively. Recombinant Sema4D, consisting of the extracellular region of Sema4D and the Fc portion of human IgG1 (Sema4D-Fc), was made as previously described (16). Human IgG, p38 MAPK inhibitor SB203580, MEK inhibitor U0126, and JNK inhibitor SP600125 were purchased from Calbiochem (San Diego, CA).

Cell cultures and immunocytochemistry

Microglial cell line GMI-6-3 (6-3 cells) were grown in MEM (Sigma-Aldrich, St Louis, MO) containing 10% FBS, 0.2% glucose, and 5 μg/ml bovine insulin. Primary microglia were prepared as described (8, 25). Mixed cells prepared from cerebrums of newborn mice were cultured in media (10% FBS-DMEM) for 14 d. Next, microglia were detached by shaking, and the detached cells were replated onto a noncoated dish. After 30 min incubation at 37°C, adherent cells were scraped, centrifuged, and replated onto poly-L-lysine–coated 35-mm dishes (for Western blotting, 2×10^5 cells/cm^2) or eight-well Lab-Tec chamber slides (for immunostaining, 1×10^4 cells/cm^2; for measurement of nitrite, 5×10^5 cells/cm^2).

For inducible NO synthase (iNOS), CD72, or plexin-B1 staining, microglia were fixed with 4% paraformaldehyde for 15 min. After blocking with 2% BSA (Sigma-Aldrich) in PBS containing Fc-block (1:20, anti-CD16/32, 2.4G2; BD Biosciences) for 30 min, cells were incubated with rabbit anti-iNOS (1:100; BD Biosciences), mouse anti-CD72 (1:100; BD Biosciences) or mouse anti–plexin-B1 (1:50; Santa Cruz Biotechnology, Santa Cruz, CA) Abs at 4°C overnight, followed by staining with FITC-conjugated goat anti-rabbit or mouse IgG Ab (1:300, Cappel, West Chester, PA). For microglial-staining, PE-conjugated rat anti-CD11b Ab (1:100; BD Biosciences) was used. Images were collected using a confocal microscope (Carl Zeiss) equipped with IMARIS software.

Measurement of nitrite

NO production by activated microglia was determined by measuring the amounts of nitrite, a stable oxidation product of NO using Griess reactions in triplicates. An aliquot of the conditioned medium was mixed with an equal volume of 1% sulfanilamide in water and 0.1% N-1-naphthylethylenediamine dihydrochloride in 5% phosphoric acid. The absorbance was determined at 550 nm. Statistical significance was analyzed using an unpaired Student t test, and $p \leq 0.05$ was considered significant.

Western blot analysis

Western blot analysis was performed as previously described (26). Cell lysates were lysed with radio-immunoprecipitation assay buffer (PBS, 1% NP-40, 0.5% sodium deoxycholate, 0.1% SDS, pH7.4) containing protease inhibitors (20 μg/ml aprotinin, 1 mM phenyl-methylsulfonyl fluoride) and 1 mM sodium orthovanadate. The same amounts of total proteins were

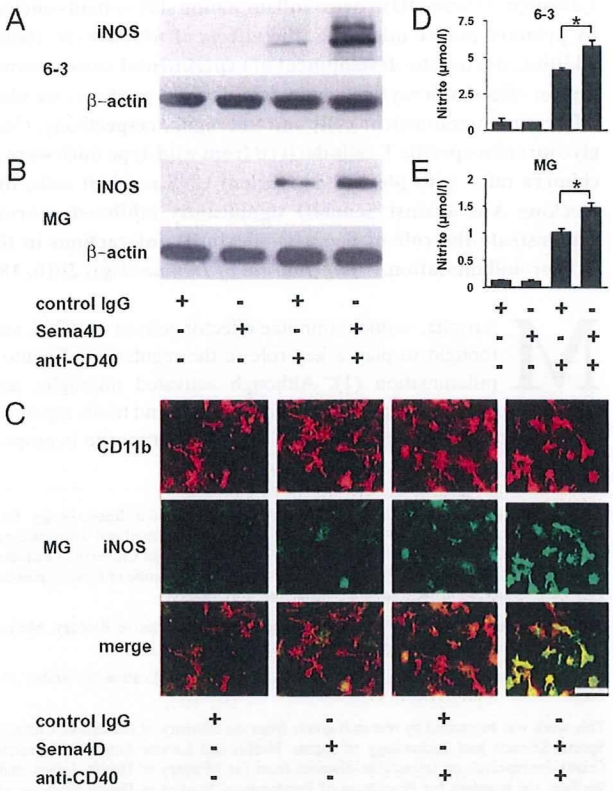

FIGURE 1. Sema4D enhances iNOS expression and NO production in microglial cells. *A* and *B*, Western blots for the iNOS expression in microglia revealed the enhancement of iNOS expression by Sema4D in a microglial cell line (6-3) (*A*) and primary microglia (MG) (*B*). INOS expression was strongly upregulated by incubation with recombinant Sema4D-Fc proteins. β-Actin was used as an internal control for Western blot analysis. *C*, Immunocytochemical analysis for iNOS expression in primary MG. The number of iNOS-positive microglia was markedly enhanced by Sema4D-Fc. CD11b was used as a microglial marker. Scale bar, 20 μm. *D* and *E*, Measurement of nitrite concentrations in the culture supernatants from microglial cell line (6-3) (*D*) and MG (*E*). Nitrite production was significantly increased by addition of Sema4D-Fc in microglia. Data are shown as mean ± SEM of triplicate wells. $*p < 0.05$. MG or microglial cell line (6-3) were incubated with indicated reagents: human IgG (20 μg/ml), Sema4D-Fc (20 μg/ml), anti-CD40 (0.5 μg/ml), plus IFN-γ (5 U/ml) for 24 h (for Western blot analysis and immunocytochemistry) or 72 h (for measurement of nitrite concentrations). The data presented are representative of three independent experiments.

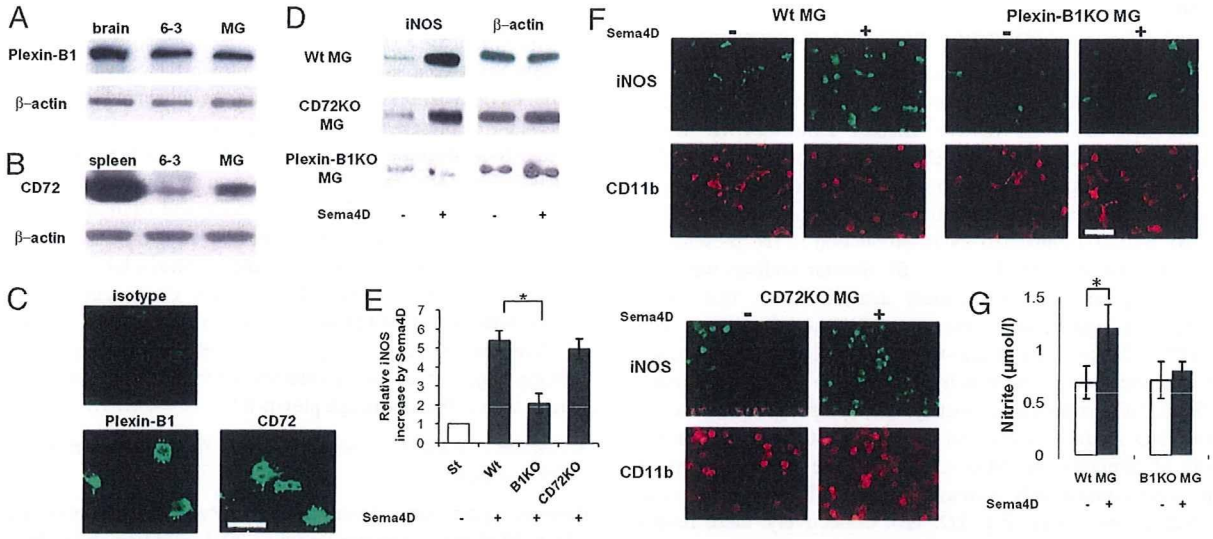

FIGURE 2. INOS and NO production by Sema4D is abolished in plexin-B1–deficient but not in CD72-deficient microglia. *A* and *B*, Western blot analysis for plexin-B1 (*A*) and CD72 (*B*) in microglia. Lysates of the brain or spleen (positive controls) were prepared. *C*, Immunocytochemical analysis for plexin-B1 and CD72 in microglial cell line (6-3). Both plexin-B1 and CD72 were expressed in microglia. Scale bar, 20 μm. *D*, Western blot analysis for iNOS expression. The induction of iNOS expression by addition of Sema4D-Fc was abolished in plexin-B1–deficient microglia, but markedly enhanced in either wild-type or CD72-deficient cells. β-Actin was used as an internal control. *E*, Relative iNOS increase by addition of Sema4D-Fc in microglia from wild-type, CD72-deficient, and plexin-B1–deficient mice. The levels of iNOS expression in microglia incubated with anti-CD40 and IFN-γ plus human IgG without Sema4D-Fc were defined as standards (St). Data are shown as mean ± SEM. $*p < 0.05$. *F*, Immunocytochemical analysis for iNOS expression in primary microglia. The number of microglia positive for iNOS was not increased by Sema4D-Fc in plexin-B1–deficient microglia, but increased in wild-type and CD72-deficient cells. Scale bar, 50 μm. *G*, Nitrite concentrations in the culture supernatants. The increase of nitrite production in the culture supernatants by addition of Sema4D-Fc was not observed in plexin-B1–deficient microglia. Data are shown as mean ± SEM of triplicate wells. $*p < 0.05$. For iNOS or NO production, cells were treated with (20 μg/ml) or without Sema4D-Fc in the presence of anti-CD40 (0.5 μg/ml) and IFN-γ (5 U/ml) for 24 h (for Western blot or immunocytochemical analysis) or 72 h (for measurement of nitrite concentrations). The data presented in are representative of at least three independent experiments.

resolved on 10% SDS-polyacrylamide gels, transferred to polyvinylidene difluoride membranes (Millipore, MA), and blotted with one of the following Abs at 4°C overnight: rabbit anti-CD72 (1:500, Santa Cruz Biotechnology), mouse anti–plexin-B1 (1:150, Santa Cruz Biotechnology), rabbit anti-iNOS (1:300, BD Biosciences), rabbit anti-phospho-ERK1/2 (1:300, Cell Signaling Technology, Danvers, MA), goat anti-MAPK (1:500, Santa Cruz Biotechnology), rabbit anti-total or phospho-JNK (Santa Cruz Biotechnology), rabbit anti-total or phospho-p38 (Santa Cruz Biotechnology) or mouse anti–β-actin (1:8000; Sigma-Aldrich) Abs. They were subsequently incubated with appropriate secondary Abs conjugated with HRP for 60 min and visualized by ECL reagents (Amersham Biosciences, Buckinghamshire, U.K.). The image of each band was captured and analyzed using Image Gauge (Fuji Film, Tokyo, Japan), which allows quantification of the bands. Statistical significance was analyzed using an unpaired Student *t* test; $p \leq 0.05$ was considered significant.

Establishment of BM chimeric mice

BM cells were isolated by flushing femur and tibia bones with HBSS. BM was filtered through a 100-μm cell strainer and cells were washed with HBSS. CD45.2 recipient mice were lethally irradiated with 950 cGy and injected i.v. with 2×10^6 CD45.1 BM cells. Engraftment took place over 6–8 wk of recovery. Mice were bled retro-orbitally to ensure 95% engraftment of blood leukocytes.

Induction of EAE

EAE was induced in 6- to 8-wk-old wild-type or plexin-B1–deficient mice on a C57BL/6 background following s.c. injection of 100 μg mouse/rat MOG_{35-55} peptides (MEVGWYRSPFSPVVHLYRNGK) emulsified in CFA, in addition to two i.v. injections of 100 ng pertussis toxin (List Laboratories, Campbell, CA) on days 0 and 2. Relapsing EAE was induced in 8-wk-old SJL mice by an s.c. immunization with 200 μl of a CFA containing 200 μg *Mycobacterium tuberculosis* H37Ra (Difco Laboratories, Sparks, MD) and 150 μg proteolipid protein $(PLP)_{139-151}$ (HSLGKWLGHPDKF) distributed over three sites on the lateral hind flanks and dorsally. All mice were monitored daily for clinical signs and were scored using a scale of 0–4 as follows: 0, no overt signs of diseases; 1, limp tail; 2, complete hind limb paralysis; 3, complete forelimb paralysis; 4, moribund state or death. Statistical significance was analyzed using an unpaired Student *t* test, and $p \leq 0.05$ was considered significant. For adoptive transfer, donor mice were immunized with MOG/CFA in the same fashion as except for no pertussis toxin. Ten days later, spleens and draining lymph nodes were collected, single-cell suspensions were prepared, and RBCs were lysed. Cells (5×10^6 cells/ml) were cultured with 40 μg/ml MOG_{35-55} peptide and 10 ng/ml recombinant mouse IL-12 (R&D Systems, Minneapolis, MN). After 3 d culture, cells were harvested and $CD4^+$ T cells were isolated by negative selection using Dynabeads (Invitrogen, Carlsbad, CA). Recipient mice irradiated sublethally (500 cGy) received cells i.v.

Immunohistochemistry

Mice were sacrificed followed by transcardiac perfusion with 4% paraformaldehyde in PBS. For Sema4D, plexin-B1, and iNOS labeling, sections (10 μm) were incubated with mouse anti–plexin-B1, mouse anti-Sema4D, or rabbit anti-iNOS Ab (1:50; Santa Cruz Biotechnology) at 4°C overnight, followed by biotin-conjugated secondary Abs (1:200, goat anti-rabbit or mouse; Vector Laboratories, Burlington, CA) for 30 min, then stained with PE-conjugated streptavidin. For double labeling, rabbit anti-IBA-1 Ab (for microglia/macrophage, 1:500; Wako, Osaka, Japan), FITC-conjugated anti-CD3 Ab (for T cells, 1:500; BD Pharmingen), and rabbit anti-GFAP Ab (for astrocytes, 1:1000; DakoCytomation, Carpinteria, CA) were used. Images were collected using a confocal microscope (Carl Zeiss, Oberkochen, Germany) equipped with IMARIS software (Bitplane AG, Zurich, Switzerland).

Mononuclear cell isolation from CNS and flow cytometry

Mice were euthanized with injection of pentobarbital, and spinal cords and brains were dissected. Both tissues were homogenized and strained through a 70-μm nylon filter (Falcon, Franklin Lakes, NJ). After centrifugation, the cell suspension was resuspended in 37% isotonic Percoll (GE Healthcare, Uppsala, Sweden) and underlayed with 70% isotonic Percoll. The gradient was centrifuged at $600 \times g$ for 25 min at room temperature. The interphase cells were collected and extensively washed before staining. For flow cytometry, the cells were stained with biotinylated anti-Sema4D, FITC-conjugated anti-CD3, APC-conjugated CD11b mAbs for 30 min at 4°C, washed, and incubated with streptavidin-PE (BD Pharmingen. San Diego, CA) for 15 min. The cells were washed and analyzed using a FACS Canto-2 using Diva software (BD Biosciences). Postacquisition analysis was performed using Flow Jo (Tomy Digital Biology, Tokyo, Japan).

Results

Sema4D enhances iNOS and NO production in microglia

To investigate the involvement of Sema4D in activation of microglia, we first examined the effects of Sema4D on the production of iNOS, one of the effector molecules in neuroinflammation (8, 27). Although iNOS production by a microglial cell line 6-3 cells or primary microglia was not detected upon incubation with recombinant Sema4D or control IgG alone (Fig. 1*A*, 1*B*), Sema4D enhanced iNOS production in the presence of anti-CD40 agonistic Ab (Fig. 1*A*, 1*B*). Similar findings were obtained using immunocytochemical analysis, such that iNOS staining was significantly upregulated by the stimulation with Sema4D in the presence of anti-CD40 agonistic Ab (Fig. 1*C*). We then examined NO production by microglia to determine whether iNOS, an NO-synthesizing isoenzyme, is responsible for the increased NO production induced by Sema4D. Consistent with the effects of Sema4D on iNOS expression, the concentrations of nitrite were considerably increased by Sema4D in both 6-3 cells and primary microglia (Fig. 1*D*, 1*E*). Collectively, these results indicate that Sema4D has enhancing effects on CD40-mediated microglial activation.

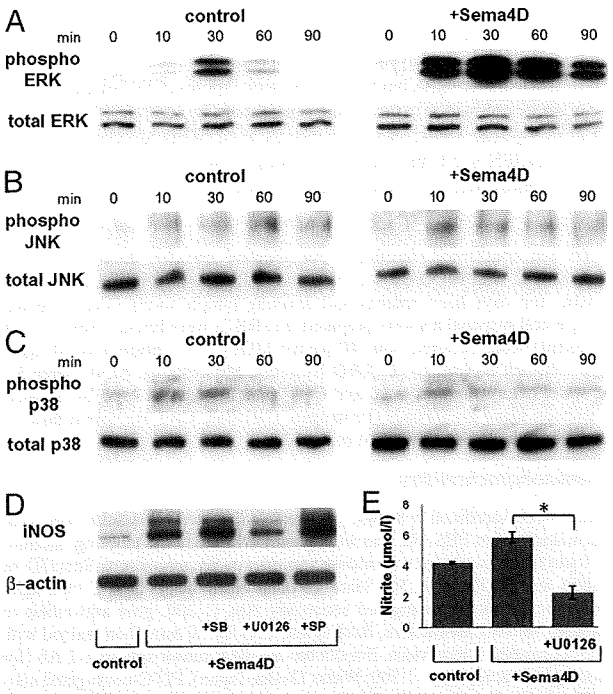

FIGURE 3. Sema4D enhances iNOS and NO production through ERK activation. *A–C*, Activation of ERK1/2, JNK, and p38 in 6-3 microglia stimulated with (*right panel*) or without (*left panel*) Sema4D-Fc. The same amounts of protein extracted from cultured cells incubated with human IgG (20 μg/ml) or Sema4D-Fc (20 μg/ml) for the indicated time in the presence of suboptimal doses of anti-CD40 plus IFN-γ were subjected to immunoblot analysis using Abs against phospho-ERK1/2 (*A*), total ERK1/2 (*A*), phospho-JNK (*B*), total JNK (*B*), phospho-p38 (*C*), and p38 (*C*). *D*, Effects of MAPK inhibitors on iNOS expression in Sema4D-treated 6-3 microglia. Cells were stimulated with Sema4D-Fc in the presence or absence of indicated kinase inhibitors for 24 h (SB203580 [SB]; p38 inhibitor, U0126; MEK1/2 inhibitor, SP600125 [SP]; JNK inhibitor). β-Actin was used as an internal control. *E*, The effect of U0126 on nitrite production from Sema4D-treated 6-3 microglia. Cells were treated with or without U0126 in the presence of suboptimal doses of anti-CD40 and IFN-γ plus Sema4D for 24 h. Data are shown as mean ± SEM of triplicate wells. $*p < 0.05$. The data are representative of three independent experiments.

Sema4D-induced iNOS and NO production is mediated through plexin-B1

Because Sema4D uses two receptors, plexin-B1 and CD72 (11), we examined their expression in microglia. As shown in Fig. 2*A–C*, the expression of plexin-B1 and CD72 proteins was observed in microglia. To address the question of which receptor is responsible for Sema4D-dependent microglial activation, we prepared microglia from plexin-B1– or CD72–deficient mice and examined their responses to Sema4D. Interestingly, the activating effects of Sema4D on microglia were significantly abolished in plexin-B1–deficient but not in CD72-deficient cells (Fig. 2*D–F*). Consistent with this, Sema4D-dependent NO production was also abolished in plexin-B1–deficient microglia (Fig. 2*G*). Collectively, these results strongly suggest that the stimulatory activities of Sema4D on microglia are mediated through plexin-B1.

Activation of ERK1/2 is responsible for Sema4D-mediated iNOS upregulation

Previous reports have shown that activation of ERK1/2 plays a key role in iNOS expression in microglia (28). In addition, the activation of other members of MAPK family, JNK and p38, is also shown to be involved in iNOS induction in glial cells (28, 29). We sought to determine whether Sema4D stimulation has an influence on ERK1/2, JNK, and p38 activation in microglia. Following stimulation with anti-CD40 agonistic Ab, phosphorylation of each kinase was observed within 10 min and then gradually declined within 90 min. Sema4D strongly enhanced ERK1/2 phosphorylation, moderately enhanced JNK phosphorylation at 10 min, and sustained ERK1/2 phosphorylation even at 90 min (Fig. 3*A*, 3*B*). However, apparent enhancement of p38 phosphorylation was not observed by the incubation with Sema4D (Fig. 3*C*).

We next examined whether the activation of these kinases induced by Sema4D was relevant to iNOS induction using several kinase inhibitors. Neither SP600125, a JNK inhibitor nor SB203580, a p38 inhibitor, did not inhibit the iNOS-upregulation by Sema4D. However, U0126, an MEK1 inhibitor, displayed an inhibitory effect on Sema4D-induced iNOS and NO production (Fig. 3*D*, 3*E*). These results suggest that enhanced activation of ERK1/2 is involved in Sema4D-mediated microglial activation.

Sema4D–plexin-B1 interactions in the CNS are involved in the pathogenesis of EAE

The in vitro findings suggest that Sema4D–plexin-B1 interactions are crucially involved in microglial activation. To address the role of Sema4D–plexin-B1 interactions during in vivo pathologic neuroinflammation, we examined the expression of Sema4D and plexin-B1 in pathogenic lesions of EAE. Although the expression of Sema4D was hardly seen in the spinal cords of control mice, it was significantly induced in infiltrating mononuclear cells of the spinal cords of mice with EAE (Fig 4*A*, 4*B*). To determine which cells expressed Sema4D in the CNS, we performed a double immunolabeling and found that $CD3^+$ T cells and a part of IBA-1^+ microglia/macrophage populations expressed Sema4D ($CD3^+$ T cells; 41 ± 2.1%, IBA-1^+ cells; 25 ± 4.1%, respectively; Fig. 4*C*, 4*D*). To further evaluate the expression of Sema4D on the surface of infiltrating mononuclear cells, we prepared mononuclear cell suspension from the brains and spinal cords of mice with EAE and analyzed them by flow cytometry. Consistent with the immunohistochemical analysis, $CD11b^+$ microglia/macrophage and $CD3^+$ T cells in the CNS of mice with EAE expressed Sema4D, whereas those from control mice did not (Fig. 4*E*, 4*F*).

Regarding plexin-B1, its expression was significantly increased in the lesions of mice with EAE, but not detected in the spinal cords of control mice (Fig. 5*A*, 5*B*). Notably, large populations of

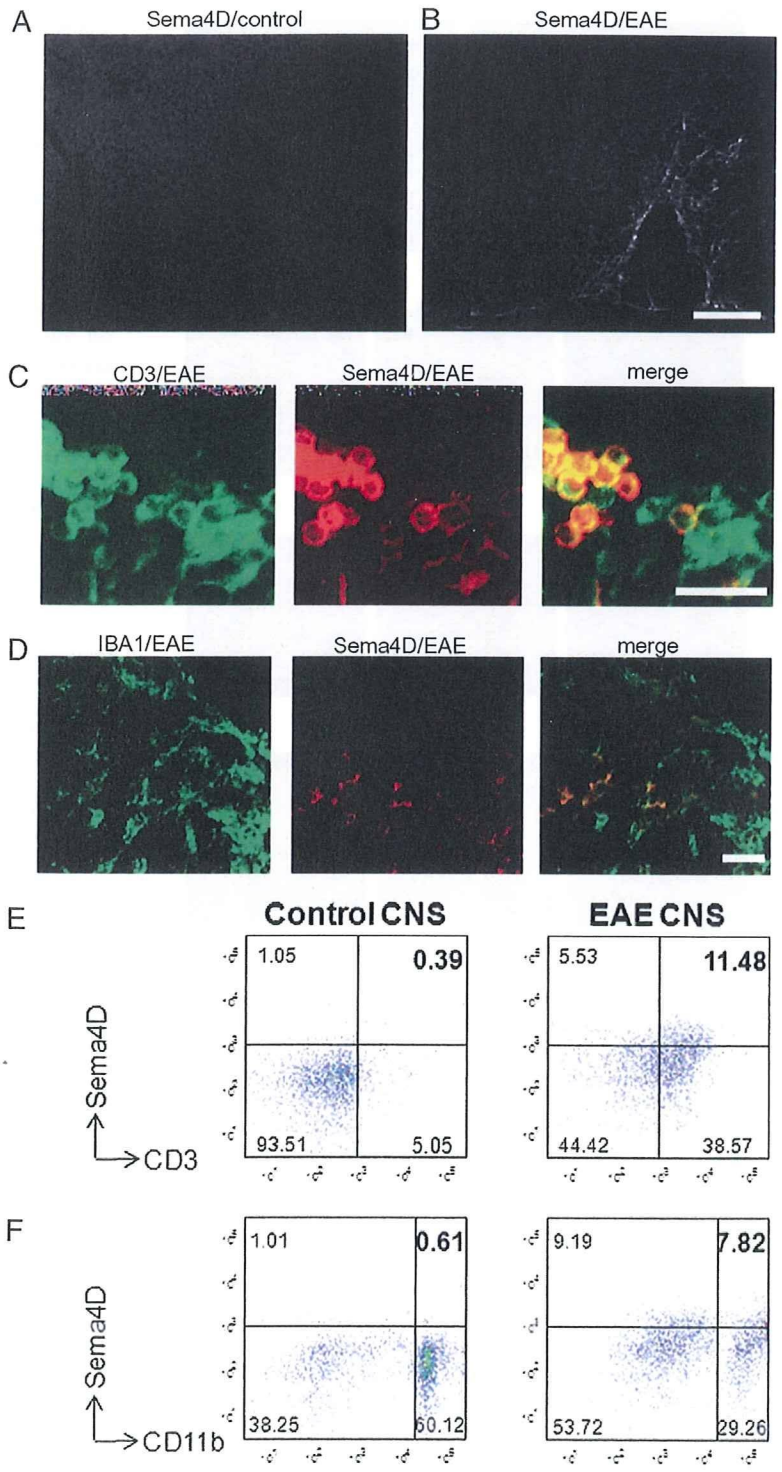

FIGURE 4. Expression of Sema4D is induced in EAE. *A* and *B*, Immunostaining of the spinal cords of control or mice with EAE. Sema4D-positive cells were not seen in the control spinal cords (*A*). By contrast, Sema4D-positive cells were abundantly observed in the white matter of EAE (*B*). Scale bar, 200 μm. *C*, A large population of CD3-positive cells were also positive for Sema4D. Scale bar, 50 μm. *D*, IBA-1–positive cells were also positive for Sema4D in mice with EAE. *E* and *F*, FACS analysis for the expression of Sema4D on $CD3^+$ or $CD11b^+$ cells in the CNS. Mononuclear cells derived from spinal cords and brains were separated by discontinuous Percoll gradient and stained with anti-Sema4D, anti-CD3, and anti-CD11b mAbs. Sema4D-positive $CD3^+$ cells or $CD11b^+$ cells were increased in the CNS of mice with EAE. EAE was induced by immunization of C57BL/6 mice with MOG_{35-55} peptides. Expression of Sema4D in the CNS was determined 7 d after the clinical onset. Age-matched nontreated mice were used as controls. Scale bar, 50 μm. All data presented are representative of analyses of three control mice with EAE.

IBA-1–positive microglia/macrophage were positive for plexin-B1 in the lesions of mice with EAE (Fig. 5*C*), whereas only a small part of CD3- or GFAP-positive cells expressed plexin-B1 (Fig. 5*D*, 5*E*). However, the expression of CD72 was not detected in the spinal cords of mice with EAE (data not shown).

We previously reported that Sema4D-deficient mice fail to develop EAE because of impaired T cell priming in the draining lymph nodes (Supplemental Fig. 1) (16). However, it has not been clarified how and to what extent Sema4D–plexin-B1 interactions in the CNS are pathologically significant during the course of EAE development. The fact that the expression of both Sema4D and plexin-B1 was induced in the lesions of EAE (Figs. 4 and 5) led us to investigate the pathologic importance of Sema4D–plexin-B1 interactions in the CNS during the course of EAE.

When we induced EAE by immunizing wild-type or plexin-B1–deficient mice with MOG_{35-55} peptides, together with pertussis toxin and CFA, plexin-B1–deficient mice displayed a relatively attenuated disease course and delayed clinical onset (Fig. 6*A*). To exclude a possibility that plexin-B1 is involved in T cell priming in the peripheral lymphoid organs, we examined the Ag-specific

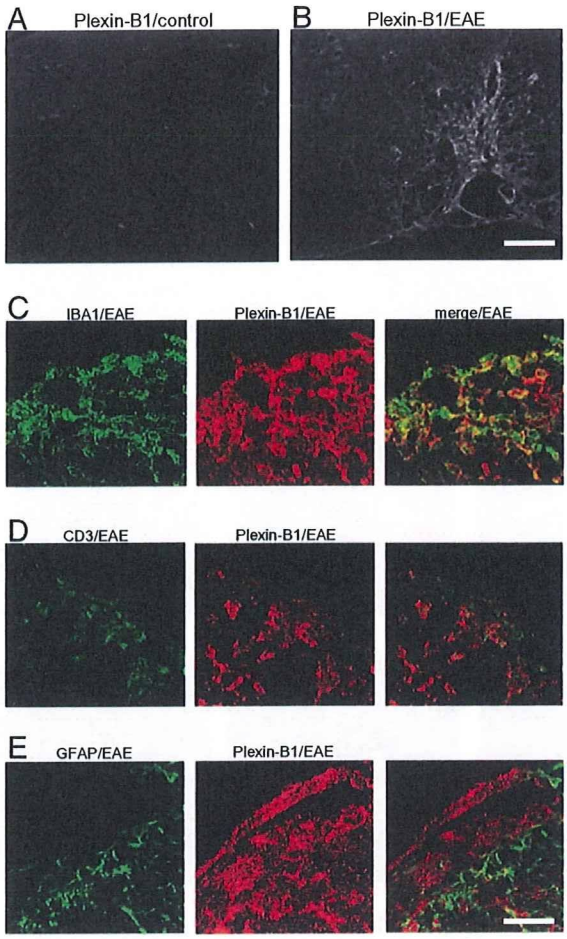

FIGURE 5. Expression of plexin-B1 is induced in EAE. *A* and *B*, Immunostaining of the spinal cords of control or mice with EAE. Plexin-B1-positive cells were not seen in the control white matter. In contrast, more plexin-B1–positive cells were observed in the white matter of EAE lesions. Scale bar, 200 μm. *C*, Most of IBA-1-positive cells were positive for plexin-B1. *D*, A small population of CD3-positive cells was positive for plexin-B1, and a large population of plexin-B1-positive cells was CD3-negative. *E*, A few GFAP-positive cells expressed plexin-B1. Scale bar, 50 μm. All data presented are representative of analyses of three control mice with EAE.

T cell priming in the draining lymph nodes in plexin-B1–deficient mice. Neither proliferation nor cytokine production in response to Ag were affected in plexin-B1–deficient mice (Supplemental Fig. 2), indicating that Sema4D–plexin-B1 interactions outside the CNS are not responsible for the resistance of EAE.

Next, to determine the pathogenic interactions between Sema4D and plexin-B1in the CNS, we adoptively transferred wild-type, MOG-specific T cells to wild-type or plexin-B1–deficient recipient mice. As is the case for active immunization, plexin-B1–deficient recipient mice displayed a diminished disease course and delayed clinical onset, compared with wild-type recipient mice (Fig. 6*B*). Consistent with the clinical course of EAE, an infiltration of mononuclear cells in the spinal cord of plexin-B1–deficient recipient mice was markedly attenuated (Fig. 6*C*). Furthermore, the expression of iNOS in the spinal cords was significantly reduced in plexin-B1–deficient recipient mice (Fig. 6*D*). To more extensively evaluate the involvement of plexin-B1 in the CNS during EAE-development, we generated BM chimera mice by transplanting wild-type CD45.1 BM cells to CD45.2 plexin-B1–deficient or wild-type mice (Wt→plexin-B1 KO, Wt→Wt), and adoptively transferred wild-type MOG-specific T cells to these chimera mice. As observed in active immunization of plexin-B1–deficient mice with MOG_{35-55} peptides, the lack of plexin-B1 expression in CNS resident cells caused a less severe disease course and delayed onset, compared with chimeric mice that express plexin-B1 in CNS resident cells (Fig. 6*E*).

Sema4D could be detected on IBA-1–positive cells in the spinal cords of mice with EAE (Fig. 4). To exclude a possible contribution of Sema4D expression in non-T cells, we adoptively transferred MOG-specific T cells into wild-type or Sema4D-deficient recipients. As shown in Fig. 6*F*, Sema4D-deficient recipient mice showed severities of EAE comparable to those observed in wild-type recipient mice, indicating that Sema4D expressed in non-T cells is not critical in the progression of EAE. Furthermore, blocking Abs against Sema4D considerably inhibited the development of relapsing EAE induced by an immunization with proteolipid protein $PLP_{139-151}$ peptides, including when they were administered after priming phases (Fig. 6*G*). Consistent with the clinical course of EAE, an infiltration of mononuclear cells in the spinal cords of mice treated with anti-Sema4D Abs was markedly attenuated (Fig. 6*H*). Collectively, these findings strongly support the notion that Sema4D–plexin-B1 interactions in the CNS are pathologically involved in the development of EAE.

Discussion

Sema4D activates microglia through plexin-B1

Activation of microglia has been shown to play a crucial role in inflammation-mediated neurologic disorders, such as multiple sclerosis and Alzheimer's disease, by producing various kinds of inflammatory effector molecules. In this study, we demonstrate that Sema4D activates microglia by increasing NO production via a plexin-B1–dependent mechanism. Further, T cell-derived Sema4D is crucially involved in the progression of EAE through interactions with plexin-B1 expressed in microglia.

In the immune system, we previously reported that Sema4D enhances CD40 signaling in B cells and DCs (15, 16). Consistent with these previous findings, we found that Sema4D promoted CD40-mediated activation of microglial cells. However, the mechanisms seem to be different between immune cells and microglia. Sema4D is known to use two types of receptors, plexin-B1 in the nervous system and CD72 in the immune system. plexin-B1 mediates Sema4D-induced axon guidance in the CNS (18), and CD72 mediates Sema4D-dependent modulation of the CD40 pathway in peripheral immune responses (15, 30). Despite the expression of CD72 on microglia, the enhancement of iNOS expression was still observed in CD72-deficient microglia. In contrast, the effects of Sema4D were significantly abolished in plexin-B1–deficient microglia (Fig. 2). These results indicate that enhancement of iNOS expression in microglia by Sema4D occurs in a CD72-independent and plexin-B1–dependent manner. It has been demonstrated that plexin-B1 displays higher affinity to Sema4D than CD72 (31). It thus appears that Sema4D preferentially binds to plexin-B1 in microglia because of its higher affinity to Sema4D rather than CD72 (31).

NO production by Sema4D is mediated via ERK pathways

An activation of MAPK family members, such as ERK and p38, has been shown to play a critical role in the regulation of iNOS and TNF-α in microglia (28, 32). It has been reported that CD40 stimulation in microglia results in an activation of Ras-MAPK pathway via phosphorylaion of Src family proteins Lck and Lyn, leading to the production of proinflammatory cytokines such as TNF-α (33). Similarly, Sema4D was reported to activate Ras-MAPK pathway downstream of plexin-B1 in neuronal cells and endothelial cells

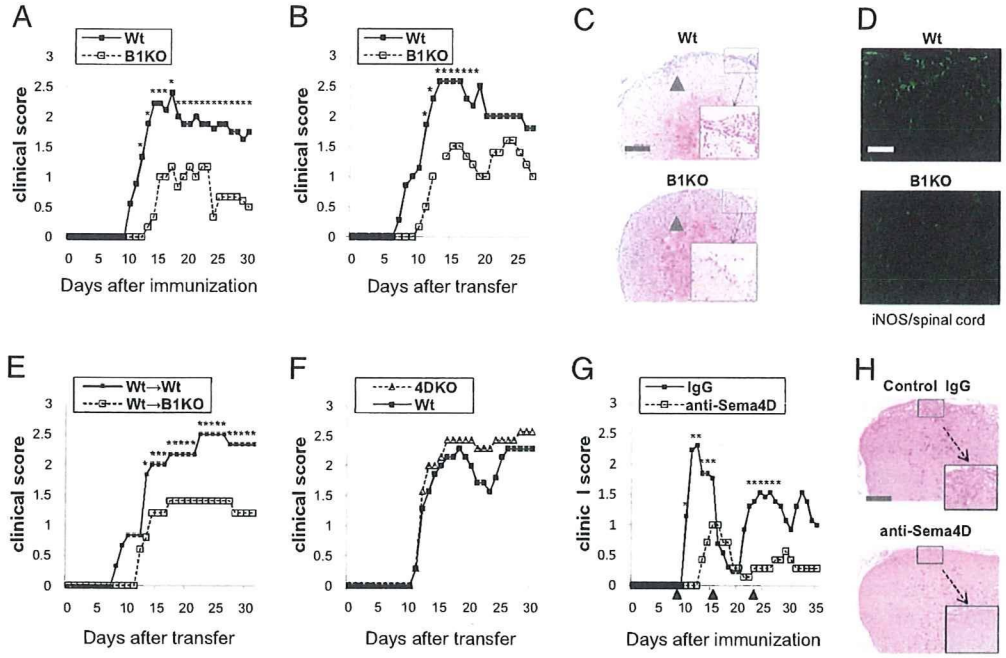

FIGURE 6. Plexin-B1–deficient mice exhibit reduced susceptibility to EAE due to the attenuated neuroinflammation. *A*, Clinical course of actively immunized EAE in plexin-B1–deficient mice. Wild-type ($n = 7$, closed squares) and plexin-B1–deficient ($n = 7$, open squares) mice were immunized with 100 μg MOG_{35-55} peptides in CFA; 100 ng of pertussis toxin was injected i.v. on days 0 and 2. The mean clinical score was calculated by averaging the scores of the mice in each group. $*p < 0.05$. *B*, Adoptive transfer of MOG-specific T cells into plexin-B1–deficient recipients induced attenuated EAE, compared with transfer into wild-type recipients. MOG-specific T cells were adoptively transferred into sublethally irradiated recipients (wild-type recipients, $n = 7$; plexin-B1–deficient recipients, $n = 8$). $*p < 0.05$. *C*, Spinal cord sections (7 d after the clinical onset) stained with H&E. The spinal cords of plexin-B1–deficient recipients had less infiltration of inflammatory mononuclear cells. Infiltrating mononuclear cells are indicated with arrowheads. The boxed areas show higher magnification. Scale bar, 300 μm. *D*, Spinal cord sections (7 d after the clinical onset) stained with anti-iNOS Ab. Reduced iNOS expression was observed in the spinal cords of plexin-B1–deficient recipients. Scale bar, 50 μm. *E*, Adoptive transfer of MOG-specific T cells into wild-type→plexin-B1–deficient BM chimeras resulted in less severe EAE, compared with transfer into wild-type→wild-type mice. BM chimeras were generated by transplanting wild-type BM cells to lethally irradiated plexin-B1–deficient or wild-type mice. Ten weeks after transplantation, MOG-specific T cells were adoptively transferred into sublethally irradiated recipients (wild-type→plexin-B1–deficient mice, $n = 6$; wild-type→wild-type mice, $n = 6$). $*p < 0.05$. *F*, Adoptive transfer of MOG-specific T cells into Sema4D-deficient recipients induced EAE similar to that induced in wild-type recipients (wild-type recipients, $n = 7$; Sema4D-deficient recipients, $n = 7$). *G*, Anti-Sema4D blocking Abs inhibited clinical progression of relapsing EAE. SJL mice were primed with $PLP_{139-151}$/CFA as described in *Materials and Methods*. Mice were treated with either anti-Sema4D (clones 5H7 and 3E9, $n = 7$) or control IgG ($n = 12$) on days 9, 16, and 23 (arrowheads). $*p < 0.05$. *H*, Spinal cord sections from relapsing EAE (30 d after the immunization) stained with H&E. The spinal cords of mice treated with anti-Sema4D Abs had less infiltration of inflammatory mononuclear cells than with control IgG. The boxed areas show higher magnification. Scale bar, 300 μm. The data presented in *A*, *B*, and *E–G* are representative of at least two independent experiments. Data presented in *C*, *D*, and *H* are representative of analyses of at least three mice in each group.

(34, 35). These findings prompted us to investigate the activation of MAPK family members, and this study provides evidence that the phosphorylation of ERK was significantly enhanced by Sema4D in concert with CD40 (Fig. 3). Furthermore, the enhancement of iNOS expression by Sema4D was inhibited by an inhibitor of ERK, but not by inhibitors of p38 or JNK (Fig. 3). These results support a role of ERK activation in the regulation of iNOS production by Sema4D in microglia. It has been reported that plexin-B1, through association with PDZ-ρ guanine nucleotide exchange factors and leukemia-associated RhoGEF, is involved in activation of RhoA in response to Sema4D (17, 36) and that ERK1/2 can be activated via plexin-B1 in neural cells and endothelial cells (34, 35). In this context, it is plausible that plexin-B1 regulates ERK1/2 signaling pathways in concert with CD40 signals. Further studies would be required to clarify the signaling mechanisms.

Interactions between Sema4D and plexin-B1 in the CNS are crucial for the progression of EAE

Consistent with our in vitro data that Sema4D–plexin-B1 interactions were involved in activation of microglia (Figs. 1 and 2), we further found that plexin-B1–deficient mice or BM chimera mice with a deficiency in plexin-B1 expression in the CNS were resistant to the development of EAE after an adoptive transfer of MOG-specific T cells (Fig. 6). It is well known that Sema4D is abundantly expressed on T cells (12). Indeed, in the pathologic lesions of EAE, Sema4D was expressed in infiltrating T cells in the spinal cords (Fig. 4), whereas plexin-B1 was expressed in microglia (Fig. 5). It thus appears that CNS- infiltrating, Sema4D-positive T cells can interact with plexin-B1–positive, CNS-resident microglia, resulting in activation of microglia during EAE progression. It is possible that BM-derived macrophages have some contribution to the neuroinflammation in EAE, because Sema4D is also expressed on cells other than T cells, such as IBA-1–positive microglia/macrophages in the spinal cords of mice with EAE (Fig. 4). However, there were not significant differences in the severity of EAE between Sema4D-deficient and wild-type recipient mice when transferred with wild-type MOG-specific T cells. This finding implies that T cell-derived Sema4D is primarily responsible for the pathogenesis of EAE through interactions with plexin-B1–expressing microglia. It is also possible that T cell-derived Sema4D has some influence on other CNS cells such as oligodendrocytes. In fact, Giraudon et al. (21) reported that T cell-derived Sema4D induces collapse of

process extension in immature oligodendrocytes and death of immature neural cells, resulting in compromised remyelination in the inflamed brain. However, plexin-B1–deficient mice displayed delayed onsets and decreased severities of EAE even at the early phase, which is difficult to explain simply with improved remyelination at the later phase of EAE. In addition, major populations of plexin-B1–positive cells were also positive for IBA-1, but negative for the oligodendrocyte marker OLIG-1 (data not shown). Collectively, these findings support the conclusion that attenuated development of EAE in plexin-B1–deficient mice is primarily due to impaired Sema4D-mediated microglial activation. However, we cannot completely exclude a possibility that Sema4D may directly injure oligodendrocytes in EAE. In addition, a possible protective effect of Sema4D in neuroinjury was recently suggested (37), although our experimental system could not reproduce such results.

In conclusion, we demonstrat that Sema4D–plexin-B1 interactions are crucially involved in activation of microglia. We also present that Sema4D is expressed in infiltrating T cells in the spinal cord of mice with EAE, whereas plexin-B1 is expressed in microglia and participates in the pathogenesis of EAE in the CNS. Furthermore, blocking Abs against Sema4D significantly inhibits neuroinflammation during EAE development. Together with our previous data that MOG-specific T cell priming is impaired in Sema4D-deficient mice (16), a blockade of Sema4D would be a valuable therapeutic target for neuroinflammatory diseases including EAE, because it can prevent the generation of encephalitogenic T cells and ameliorate inflammation even after clinical onset.

Acknowledgments

We thank T. Yazawa for technical support.

Disclosures

The authors have no financial conflicts of interests.

References

1. Ransohoff, R. M., and V. H. Perry. 2009. Microglial physiology: unique stimuli, specialized responses. *Annu. Rev. Immunol.* 27: 119–145.
2. Heppner, F. L., M. Greter, D. Marino, J. Falsig, G. Raivich, N. Hövelmeyer, A. Waisman, T. Rülicke, M. Prinz, J. Priller, et al. 2005. Experimental autoimmune encephalomyelitis repressed by microglial paralysis. *Nat. Med.* 11: 146–152.
3. Jack, C., F. Ruffini, A. Bar-Or, and J. P. Antel. 2005. Microglia and multiple sclerosis. *J. Neurosci. Res.* 81: 363–373.
4. Ponomarev, E. D., L. P. Shriver, and B. N. Dittel. 2006. CD40 expression by microglial cells is required for their completion of a two-step activation process during central nervous system autoimmune inflammation. *J. Immunol.* 176: 1402–1410.
5. Tan, J., T. Town, D. Paris, T. Mori, Z. Suo, F. Crawford, M. P. Mattson, R. A. Flavell, and M. Mullan. 1999. Microglial activation resulting from CD40-CD40L interaction after β-amyloid stimulation. *Science* 286: 2352–2355.
6. Becher, B., B. G. Durell, A. V. Miga, W. F. Hickey, and R. J. Noelle. 2001. The clinical course of experimental autoimmune encephalomyelitis and inflammation is controlled by the expression of CD40 within the central nervous system. *J. Exp. Med.* 193: 967–974.
7. Gerritse, K., J. D. Laman, R. J. Noelle, A. Aruffo, J. A. Ledbetter, W. J. Boersma, and E. Claassen. 1996. CD40-CD40 ligand interactions in experimental allergic encephalomyelitis and multiple sclerosis. *Proc. Natl. Acad. Sci. U.S.A.* 93: 2499–2504.
8. Okuno, T., Y. Nakatsuji, A. Kumanogoh, M. Moriya, H. Ichinose, H. Sumi, H. Fujimura, H. Kikutani, and S. Sakoda. 2005. Loss of dopaminergic neurons by the induction of inducible nitric oxide synthase and cyclooxygenase-2 via CD 40: relevance to Parkinson's disease. *J. Neurosci. Res.* 81: 874–882.
9. Kolodkin, A. L., D. J. Matthes, and C. S. Goodman. 1993. The semaphorin genes encode a family of transmembrane and secreted growth cone guidance molecules. *Cell* 75: 1389–1399.
10. Zhou, Y., R. A. Gunput, and R. J. Pasterkamp. 2008. Semaphorin signaling: progress made and promises ahead. *Trends Biochem. Sci.* 33: 161–170.
11. Suzuki, K., A. Kumanogoh, and H. Kikutani. 2008. Semaphorins and their receptors in immune cell interactions. *Nat. Immunol.* 9: 17–23.
12. Bougeret, C., I. G. Mansur, H. Dastot, M. Schmid, G. Mahouy, A. Bensussan, and L. Boumsell. 1992. Increased surface expression of a newly identified 150-kDa dimer early after human T lymphocyte activation. *J. Immunol.* 148: 318–323.
13. Shi, W., A. Kumanogoh, C. Watanabe, J. Uchida, X. Wang, T. Yasui, K. Yukawa, M. Ikawa, M. Okabe, J. R. Parnes, et al. 2000. The class IV semaphorin CD100 plays nonredundant roles in the immune system: defective B and T cell activation in CD100-deficient mice. *Immunity* 13: 633–642.
14. Tamagnone, L., S. Artigiani, H. Chen, Z. He, G. I. Ming, H. Song, A. Chedotal, M. L. Winberg, C. S. Goodman, M. Poo, et al. 1999. Plexins are a large family of receptors for transmembrane, secreted, and GPI-anchored semaphorins in vertebrates. *Cell* 99: 71–80.
15. Kumanogoh, A., C. Watanabe, I. Lee, X. Wang, W. Shi, H. Araki, H. Hirata, K. Iwahori, J. Uchida, T. Yasui, et al. 2000. Identification of CD72 as a lymphocyte receptor for the class IV semaphorin CD100: a novel mechanism for regulating B cell signaling. *Immunity* 13: 621–631.
16. Kumanogoh, A., K. Suzuki, E. Ch'ng, C. Watanabe, S. Marukawa, N. Takegahara, I. Ishida, T. Sato, S. Habu, K. Yoshida, et al. 2002. Requirement for the lymphocyte semaphorin, CD100, in the induction of antigen-specific T cells and the maturation of dendritic cells. *J. Immunol.* 169: 1175–1181.
17. Swiercz, J. M., R. Kuner, J. Behrens, and S. Offermanns. 2002. Plexin-B1 directly interacts with PDZ-RhoGEF/LARG to regulate RhoA and growth cone morphology. *Neuron* 35: 51–63.
18. Oinuma, I., Y. Ishikawa, H. Katoh, and M. Negishi. 2004. The Semaphorin 4D receptor Plexin-B1 is a GTPase activating protein for R-Ras. *Science* 305: 862–865.
19. Czopik, A. K., M. S. Bynoe, N. Palm, C. S. Raine, and R. Medzhitov. 2006. Semaphorin 7A is a negative regulator of T cell responses. *Immunity* 24: 591–600.
20. Suzuki, K., T. Okuno, M. Yamamoto, R. J. Pasterkamp, N. Takegahara, H. Takamatsu, T. Kitao, J. Takagi, P. D. Rennert, A. L. Kolodkin, et al. 2007. Semaphorin 7A initiates T-cell-mediated inflammatory responses through alpha1beta1 integrin. *Nature* 446: 680–684.
21. Giraudon, P., P. Vincent, C. Vuaillat, O. Verlaeten, L. Cartier, A. Marie-Cardine, M. Mutin, A. Bensussan, M. F. Belin, and L. Boumsell. 2004. Semaphorin CD100 from activated T lymphocytes induces process extension collapse in oligodendrocytes and death of immature neural cells. *J. Immunol.* 172: 1246–1255.
22. Friedel, R. H., G. Kerjan, H. Rayburn, U. Schüller, C. Sotelo, M. Tessier-Lavigne, and A. Chédotal. 2007. Plexin-B2 controls the development of cerebellar granule cells. *J. Neurosci.* 27: 3921–3932.
23. Friedel, R. H., A. Plump, X. Lu, K. Spilker, C. Jolicoeur, K. Wong, T. R. Venkatesh, A. Yaron, M. Hynes, B. Chen, et al. 2005. Gene targeting using a promoterless gene trap vector ("targeted trapping") is an efficient method to mutate a large fraction of genes. *Proc. Natl. Acad. Sci. USA* 102: 13188–13193.
24. Pan, C., N. Baumgarth, and J. R. Parnes. 1999. CD72-deficient mice reveal nonredundant roles of CD72 in B cell development and activation. *Immunity* 11: 495–506.
25. Kanzawa, T., M. Sawada, K. Kato, K. Yamamoto, H. Mori, and R. Tanaka. 2000. Differentiated regulation of allo-antigen presentation by different types of murine microglial cell lines. *J. Neurosci. Res.* 62: 383–388.
26. Okuno, T., Y. Nakatsuji, A. Kumanogoh, K. Koguchi, M. Moriya, H. Fujimura, H. Kikutani, and S. Sakoda. 2004. Induction of cyclooxygenase-2 in reactive glial cells by the CD40 pathway: relevance to amyotrophic lateral sclerosis. *J. Neurochem.* 91: 404–412.
27. Jana, M., X. Liu, S. Koka, S. Ghosh, T. M. Petro, and K. Pahan. 2001. Ligation of CD40 stimulates the induction of nitric-oxide synthase in microglial cells. *J. Biol. Chem.* 276: 44527–44533.
28. Bhat, N. R., P. Zhang, J. C. Lee, and E. L. Hogan. 1998. Extracellular signal-regulated kinase and p38 subgroups of mitogen-activated protein kinases regulate inducible nitric oxide synthase and tumor necrosis factor-α gene expression in endotoxin-stimulated primary glial cultures. *J. Neurosci.* 18: 1633–1641.
29. Han, I. O., K. W. Kim, J. H. Ryu, and W. K. Kim. 2002. p38 mitogen-activated protein kinase mediates lipopolysaccharide, not interferon-γ, -induced inducible nitric oxide synthase expression in mouse BV2 microglial cells. *Neurosci. Lett.* 325: 9–12.
30. Wang, X., A. Kumanogoh, C. Watanabe, W. Shi, K. Yoshida, and H. Kikutani. 2001. Functional soluble CD100/Sema4D released from activated lymphocytes: possible role in normal and pathologic immune responses. *Blood* 97: 3498–3504.
31. Kumanogoh, A., and H. Kikutani. 2001. The CD100-CD72 interaction: a novel mechanism of immune regulation. *Trends Immunol.* 22: 670–676.
32. Han, I. O., H. S. Kim, H. C. Kim, E. H. Joe, and W. K. Kim. 2003. Synergistic expression of inducible nitric oxide synthase by phorbol ester and interferon-γ is mediated through NF-kappaB and ERK in microglial cells. *J. Neurosci. Res.* 73: 659–669.
33. Tan, J., T. Town, M. Saxe, D. Paris, Y. Wu, and M. Mullan. 1999. Ligation of microglial CD40 results in p44/42 mitogen-activated protein kinase-dependent TNF-α production that is opposed by TGF-β 1 and IL-10. *J. Immunol.* 163: 6614–6621.
34. Aurandt, J., W. Li, and K. L. Guan. 2006. Semaphorin 4D activates the MAPK pathway downstream of plexin-B1. *Biochem. J.* 394: 459–464.
35. Basile, J. R., J. Gavard, and J. S. Gutkind. 2007. Plexin-B1 utilizes RhoA and ρ kinase to promote the integrin-dependent activation of Akt and ERK and endothelial cell motility. *J. Biol. Chem.* 282: 34888–34895.
36. Swiercz, J. M., R. Kuner, and S. Offermanns. 2004. Plexin-B1/RhoGEF-mediated RhoA activation involves the receptor tyrosine kinase ErbB-2. *J. Cell Biol.* 165: 869–880.
37. Toguchi, M., D. Gonzalez, S. Furukawa, and S. Inagaki. 2009. Involvement of Sema4D in the control of microglia activation. *Neurochem, Int.* 55: 573–580.

A midline switch of receptor processing regulates commissural axon guidance in vertebrates

Homaira Nawabi,[1,4] Anne Briançon-Marjollet,[1,4] Christopher Clark,[1] Isabelle Sanyas,[1] Hyota Takamatsu,[2] Tatsusada Okuno,[2] Atsushi Kumanogoh,[2] Muriel Bozon,[1] Kaori Takeshima,[3] Yutaka Yoshida,[3] Frédéric Moret,[1] Karima Abouzid,[1] and Valérie Castellani[1,5]

[1]University of Lyon, University of Lyon 1, Claude Bernard Lyon1, CGMC, UMR, CNRS 5534, F-69000 Lyon, France; [2]Department of Immunology, Research Institute for Microbial Diseases, Osaka University, Osaka, 565-0871, Japan; [3]Division of Developmental Biology, Cincinnati Children's Hospital Medical Center, Cincinnati, Ohio 45229, USA

Commissural axon guidance requires complex modulations of growth cone sensitivity to midline-derived cues, but underlying mechanisms in vertebrates remain largely unknown. By using combinations of ex vivo and in vivo approaches, we uncovered a molecular pathway controlling the gain of response to a midline repellent, Semaphorin3B (Sema3B). First, we provide evidence that Semaphorin3B/Plexin-A1 signaling participates in the guidance of commissural projections at the vertebrate ventral midline. Second, we show that, at the precrossing stage, commissural neurons synthesize the Neuropilin-2 and Plexin-A1 Semaphorin3B receptor subunits, but Plexin-A1 expression is prevented by a calpain1-mediated processing, resulting in silencing commissural responsiveness. Third, we report that, during floor plate (FP) in-growth, calpain1 activity is suppressed by local signals, allowing Plexin-A1 accumulation in the growth cone and sensitization to Sema3B. Finally, we show that the FP cue NrCAM mediates the switch of Plexin-A1 processing underlying growth cone sensitization to Sema3B. This reveals pathway-dependent modulation of guidance receptor processing as a novel mechanism for regulating guidance decisions at intermediate targets.

[*Keywords*: Axon guidance; midline crossing; semaphorin; calpain; commissural neurons]

Supplemental material is available at http://www.genesdev.org.

Received June 5, 2009; revised version accepted December 18, 2009.

The developing neuronal projections navigate along highly diverse environments and manage complex pathway choices to reach their specific target tissues. Axon trajectories are specified by multiple cues, and guidance decisions crucially depend on regulatory mechanisms controlling in time and space the expression, distribution, and activity of the guidance machinery, including ligands, receptors, and signaling effectors (Yu and Bargmann 2001). The pathfinding of long-distance projections proceeds in successive stages, with regularly positioned sources of attractants keeping axons in appropriate routes, referred to as intermediate targets. For example, in vertebrates, groups of neurons in the CNS send axon projections that navigate through a key intermediate target, the floor plate (FP), in which they cross the midline. In the developing spinal cord, commissural neurons reside in the dorsal horn, and their axons navigate ventromedially to cross the midline and turn rostrally, extending along longitudinal pathways. Axon tracts then contact various spinal and higher-center neurons to establish circuits participating in the left–right control of sensory modalities and motor behaviors (Colamarino and Tessier-Lavigne 1995). Extensive studies established that Netrins, Semaphorins, IgSFCAMs, Slits, and various morphogens combine contact and diffusible attractive and repulsive effects to control commissural axon pathfinding (Augsburger et al. 1999; Garbe and Bashaw 2004; Dickson and Gilestro 2006).

A key issue that long-distance projections have to solve is how to leave an intermediate target. One possibility is that, among the guidance cues to which they are exposed, commissural axons first perceive attractants, thus being guided toward the intermediate target, and second repellents during in-growth, thereby receiving instructions for intermediate target exit. Accordingly, spinal commissural axons are attracted to the FP by Netrins and Shh, but then lose their responsiveness to Netrins and become sensitive to midline-derived repellents of the Slit, Semaphorin, and Ephrin families (Kidd et al. 1998; Brose et al. 1999; Zou et al. 2000; Imondi and Kaprielian 2001). Very

[4]These authors contributed equally to this work.
[5]Corresponding author.
E-MAIL castellani@cgmc.univ-lyon1.fr; FAX 33-0472442685.
Article is online at http://www.genesdev.org/cgi/doi/10.1101/gad.542510.
Freely available online through the *Genes & Development* Open Access option.